VOT 71803

PHOTOCATALYTIC OXIDATION OF VOLATILE ORGANIC COMPOUNDS (VOC's) IN AIR USING TITANIUM DIOXIDE (TiO_2) BASED MATERIALS

MOHD YUSUF BIN OTHMAN
WAN AZELEE BIN WAN ABU BAKAR
NOOR KHAIDA WATI BTE MOHD SAIYUDI

FAKULTI SAINS
UNIVERSITI TEKNOLOGI MALAYSIA

2003

ACKNOWLEDGEMENTS

The authors wished to thank the Ministry of Science, Technology and Environment (MOSTE) Malaysia, Research Management Centre (RMC), UTM and Faculty of Science Universiti Teknologi Malaysia, Skudai.

ABSTRACT

Heterogeneous photocatalytic oxidation is a promising technique for the removal of volatile organic pollutants (VOCs). It allows the oxidation of gaseous VOCs into carbon dioxide and water in the presence of a semiconductor catalyst and UV light. Titanium dioxide (TiO_2) represents one of the most efficient photocatalyst. It is chemically stable, non-toxic and low cost. However, the photoexcitation processes of pure TiO_2 is only active in the ultra violet fraction of the solar irradiation and although, TiO_2 can treat a wide range of VOCs, the effectiveness of the process for pollution abatement is still low. Doping TiO_2 with metal ions was considered as an alternative method to improve TiO_2 photocatalytic properties. In this study, transparent TiO_2 thin films were prepared using the sol-gel and dip-coating method. Various ratios of doped TiO_2 thin films were also prepared using Cr^{3+}, Fe^{3+}, Cu^{2+}, Ni^{2+}, Co^{2+}, Zn^{2+}, Mn^{2+} and Ag^{+}. All photodegradation processes were conducted in a home built glass reactor. Photocatalytic oxidation of benzene using various ratios of metal-doped TiO_2 showed an optimum dopant to metal ion ratio. This shows that dopant concentration affect the photocatalytic activity of TiO_2. Photodegradation of benzene, toluene, *m*-xylene, acetone and tetrachloroethylene (TeCE) were conducted using the catalyst with the optimum ratio. It was noted that the photoactivity of doped TiO_2 substantially depends not only on the type and concentration of dopant but also VOCs. Dopants affect the photoreactivity of TiO_2 by acting either as electron/hole trap or electron-hole recombination center. High photocatalytic degradation of all the VOCs was observed with pure TiO_2. However adding Fe^{3+} and Ag^{+} into TiO_2 increased the photodegradation of benzene and acetone while Zn^{2+} in toluene and *m*-xylene degradation. Dopants such as Cr^{3+}, Co^{2+}, Cu^{2+}, Ni^{2+} and Mn^{2+} decreased the photoreactivity of TiO_2 in the photodegradation of all VOCs under studied. Dopants have no effect in TeCE degradation. TeCE shows highest degradation compared to the non-chlorinated hydrocarbon. This was attributed to the participation of chlorine radical, which induced a chain reaction mechanism. Mechanistic studies using GCMS shows that the primary species in the photodegradation of benzene and acetone is the hydroxyl radical while in toluene photodegradation, direct reaction of photogenerated electron and toluene could be the possible pathway. Structural and optical properties of the thin films were characterized using XRD, SEM/EDAX, XPS and UV-Vis. All thin films showed TiO_2 anatase phase. Surface species such as Ti^{4+}, surface hydroxyl and physically adsorbed water increased the photoreactivity of TiO_2. All thin film exhibited homogenously distributed pores. Dopants such as Zn, Mn and Ag shift the absorption edge of TiO_2 into the visible region indicating reduced band gap energy.

ABSTRAK

Pengoksidaan fotopemangkinan heterogen merupakan kaedah yang berupaya mengurangkan kandungan bahan mudah meruap (VOCs) di udara. Kaedah ini melibatkan pengoksidaan VOCs kepada karbon dioksida dan air dengan menggunakan mangkin semikonduktor dan cahaya UL. Titanium dioksida merupakan fotomangkin yang sangat berkesan kerana kestabilan kimia, tidak toksik dan murah. Bagaimanapun, dalam pancaran solar, hanya kawasan UL adalah aktif dalam proses fotopengujaan TiO_2 tulen. Walaupun TiO_2 boleh merawat sejumlah besar VOCs, keberkesanan proses ini dalam mengawal pencemaran udara masih rendah. Kaedah mendop TiO_2 dengan ion logam telah dipertimbangkan sebagai kaedah alternatif untuk meningkatkan sifat mangkinfoto TiO_2. Dalam kajian ini saput tipis TiO_2 telah disediakan dengan menggunakan kaedah sol-gel dan celup angkat. Saput tipis dengan berbagai nisbah bahan dop juga disediakan menggunakan ion Cr^{3+}, Fe^{3+}, Cu^{2+}, Ni^{2+}, Co^{2+}, Zn^{2+}, Mn^{2+} dan Ag^{+}. Semua proses fotodegradasi telah dijalankan di dalam reaktor kaca. Pengoksidaan fotomangkin benzena menggunakan semua mangkin menunjukan satu nilai optimum bahan pendop terhadap TiO_2. Nilai ini menunjukkan bahawa aktiviti fotomangkin TiO_2 bergantung kepada kepekatan bahan pendop. Kereaktifan saput tipis telah dinilai melalui fotodegradasi benzena, toluena, m-silena, aseton dan tetrakloroetilena (TeCE) menggunakan mangkin dengan nisbah optimum. Diperhatikan bahawa fotoaktiviti TiO_2 berpendop bergantung kepada jenis dan kepekatan pendop dan VOCs. Dopan mempengaruhi fotoreaktiviti TiO_2 dengan bertindak sebagai perangkap e^{-}/h^{+} atau sebagai pusat pengabungan e^{-}/h^{+}. Fotodegradasi VOCs adalah tinggi menggunakan TiO_2 tulen. Tetapi penambahan Fe^{3+} dan Ag^{+} ke dalam TiO_2 meningkatkan fotoreaktiviti TiO_2 dalam degradasi benzena dan aseton manakala Zn^{2+} untuk toluena dan m-silena. Dopan seperti Cr^{3+}, Cu^{2+}, Ni^{2+}, Co^{2+}, dan Mn^{2+} menurunkan aktiviti TiO_2. Fotodegradasi TeCE bagaimanapun tidak dipengaruhi oleh dopan. Fotodegradsi TeCE adalah sangat tinggi berbanding sebatian hidrocarbon tanpa klorin. Degradasi TeCE yang tinggi adalah berpunca daripada penglibatan radikal klorin yang menyuntik satu mekanisme rantai. Analisis bahan perantaran menggunakan GC-MS menunjukkan bahawa sepsis utama dalam fotodegradasi benzena dan asetone adalah radikal hidroksil manakala dalam fotodegradasi toluene tindak balas langsung elektron terhasil foto dengan toluene mungkin merupakan laluan tindak balas. Sifat struktur dan optik saput tipis dicirikan menggunakan XRD, SEM/EDAX, XPS, dan UV-Vis. Semua mangkin saput tipis menunjukkan fasa anatas. Kewujudan fasa rutil menyebabkan penurunan fotoaktiviti TiO_2. Spesis permukaan seperti Ti^{4+}, hidrosil dan air meningkatkan fotoaktiviti TiO_2. Semua saput tipis menunjukkan liang yang tersebar secara homogen. Bahan pendop seperti Zn^{2+}, Mn^{2+} dan Ag^{+} mengubah penyerapan TiO_2 ke kawasan nampak yang menunjukkan pengurangan tenaga luang jalur.

TABLE OF CONTENTS

CHAPTER III: EXPERIMENTAL

CHAPTER IV: RESULTS AND DISCUSSION

LIST OF TABLES

LIST OF FIGURES

CHAPTER 1

1.0 INTRODUCTION

Volatile organic compounds (VOCs) are an important class of air pollutants, which are considered together with nitrogen oxides, sulfur oxides and particulates as the most important anthropogenic pollutants generated in urban and industrial areas (Avila, 1998). The term VOCs is used to identify all compounds containing carbon and present in the atmosphere, with the exception of elemental carbon, carbon monoxide and carbon dioxide (Augugliaro, 1999). VOCs are defined as having a boiling point that ranges between 50°C and 260°C (Jones, 1999). Their low boiling point means that they will readily off-gas vapors into the air at ambient temperatures. VOCs include a wide range of substances with diverse effects. Some are considered toxic and pose a greater threat to human health and the environment, such as benzene and toluene, whose emissions are associated primarily with the production, distribution and marketing of gasoline. In highly airtight houses that have little ventilation, various kinds of volatile organic compounds are released from adhesives and preservatives used in house-building materials or from furniture. The accumulations of these compounds in the airtight room can leads to the discomfort of the inhabitant and health-related complains.

Exposure to VOCs can result in both acute and chronic health effects. It is possible that asthmatics and other individuals with prior respiratory complaints may be particularly susceptible to low-dose VOCs exposures (Norback, 1995). At high concentrations, many VOCs are potent narcotics, and can depress the central nervous system (Jones, 1999). Exposures can also lead to irritation of the eyes and respiratory tract, and cause sensitization reactions involving the eyes, skin and lungs. Cancer have been associated with with exposure to high concentration of several VOCs such as, benzene, p-dichlorobenzene, chloroform, methylene chloride and carbon tetrachloride (Wallace, 1991).

As a result of all these problems, VOCs have drawn considerable attention in the last decade. Currently there is a great deal of interest in developing processes, which can destroy these compounds. Since a large number of the VOCs are oxidizable, chemical oxidation process can be looked upon as a viable method.

Photocatalytic oxidation for the removal of contaminants or pollutants from air is a growing research area and appears to be a promising process for the remediation of air and groundwater polluted by VOCs. Gas-solid heterogeneous photocatalytic oxidation has been previously demonstrated for alkanes, alcohols, aldehydes, ketones, aromatics and inorganics (Dibble, 1990; Peral, 1992; Sauer, 1994; Fu, 1995). Photocatalysis is thus established as a potential air treatment and purification technology because of its broad application to common oxidizable air contaminants. Attractive advantages with photocatalysis for air treatment and purification are operational at ambient temperatures and pressure, the use of molecular oxygen as the oxidant and final oxidation products that are usually innocuous (CO_2 and H_2O for oxidation of small hydrocarbons and HCl for compounds containing chlorine). The commercial prospects for photocatalytic air treatment and purification are due to their low capital and operational cost.

1.1 Heterogeneous Photocatalysis

Heterogeneous photocatalysis is an oxidation technique that could be successfully used for the oxidation of organic pollutant either in the aqueous or gas phase. Called "advanced oxidation processes" (AOP) these techniques use a highly active redox reagent to bring about the complete mineralization of all atoms present in an organic pollutant. In recent years much attention has been paid to the reactions that take place on the illuminated surface of semiconductor metal oxides such as TiO_2, ZnO, WO_3, SnO etc. Among these, TiO_2 is the most commonly used photocatalyst.

Activation of the semiconductor photocatalyst is achieved through the absorption of a photon of ultra-bandgap energy, which results in the promotion of an electron, e^- from the valence band to the conduction band, with the concomitant generation of a hole, h^+ in the valence band. This highly reactive e^- - h^+ pairs, after

migration to the solid surface may undergo electron-transfer processes with adsorbates or recombine. The photogenerated electrons can reduced an electron acceptor and the photogenerated holes can oxidized an electron donor. For a semiconductor photocatalyst to be efficient, the different interfacial electron processes involving e^- and h^+ must compete effectively with the major deactivation processes involving e^- - h^+ recombination.

Once excitation occurs across the band gap there is a sufficient lifetime, in the nanosecond regime (Rothenberger, 1985) for the created electron-hole pair to undergo charge transfer to adsorbed species on the semiconductor surface from solution or gas phase contact. If the scavenger or surface defects are present to trap the electron or holes, e^- - h^+ recombination can be prevented and the subsequent oxidation and reduction processes caused by electrons and holes may be enhanced (Park, 1999).

1.2 Titanium Dioxide

Titanium (IV) oxide, TiO_2, is found in many mineral forms and is the fourth most abundant metallic mineral in the earth's crust. As such, it is readily available and inexpensive to procure. Commonly, it is used as an alloying agent in the aerospace and shipbuilding industries, for strength and high corrosion resistance. This unassuming semiconductor displays photocatalytic ability when exposed to light. To show full catalytic potential, TiO_2 requires both oxygen and water, both of which are abundant in air. Photons impinging on TiO_2 dislodge electrons, creating holes and free electrons. The holes and free electrons oxidize water and oxygen, respectively, to form hydroxyl and superoxide radicals, both ruthless bond cleavers.

TiO_2 propensity for oxidation has been known for sometime. TiO_2 has been demonstrated to complete the decomposition of a large number of organic compounds. A crucial advantage with TiO_2 is that the conduction-band electrons have considerable reducing power and can be used to reduced pollutant directly. The species responsible for the organic compounds oxidation in a photocatalytic reaction is the hydroxyl radical (•OH). This highly reactive species is formed when h^+ is trapped by the absorbed hydroxyl ion or water (Equation (1.1) and (1.2)).

$$h^+ + H_2O \rightarrow \bullet OH + H^+ \quad (1.1)$$

$$h^+ + 2OH^- \rightarrow \bullet OH + OH^- \quad (1.2)$$

The hydroxyl radical is also formed when adsorbed oxygen molecules react with the conduction band electron, forming the superoxide radical as in Equation (1.3) and (1.4). The super oxide (O_2^-) formed is an effective oxygenated agent that attacks neutral substrates and surface-adsorbed radicals and/or radical ions (Fox, 1993).

$$e^- + O_2 \rightarrow \bullet O_2^- \quad (1.3)$$

$$\bullet O_2^- + H^+ \rightarrow HO_2\bullet \quad (1.4)$$

$$2HO_2\bullet \rightarrow O_2 + H_2O_2 \quad (1.5)$$

or

$$HO_2\bullet + e^- + H^+ \rightarrow H_2O_2 \quad (1.6)$$

$$H_2O_2 + O_2^- \rightarrow OH^- + \bullet OH + O_2 \quad (1.7)$$

The reaction between the $HO_2\bullet$ radicals, produce H_2O_2 that will consequently react with either the $\bullet O_2^-$ or e^-, forming the •OH radicals. Oxidation of organic substrates may occur either indirect oxidation via the surface-bound hydroxyl radical (i.e. a trapped hole at the particle surface) or directly via the valence-band hole before it is trapped either within the particle or the particle surface (Hoffman, 1995).

1.3 Dopants

The photocatalytic properties of titanium dioxide semiconductor are well established, band gap excitation of TiO_2 leads to the generation of electron/hole pairs. Photocatalytic efficiency of TiO_2 however depends, in part, upon the relative degree of branching of the reactive electron/hole pairs into interfacial charge-transfer reactions. In order to enhance interfacial charge-transfer reactions, the properties of TiO_2 have been modified by selective surface treatments. The presence of metal ion dopants in TiO_2 crystalline matrix significantly influences photoreactivity, charge carrier recombination rates and interfacial electron-transfer rate by acting as an electron (or hole) trap (Choi, 1994).

Doping implies incorporation of a foreign cation into the catalyst matrix of the parent metal oxide (Karakitsou, 1993). From a chemical point of view, TiO_2 doping is equivalent to the introduction of defect sites into the semiconductor lattice (Fox, 1993). A wide range of metal ions in particular transition metal ions, have been used as dopants. Doping titania with metal transition ions was envisaged as a good tool to improved photocatalytic properties, principally because an enhancement of interfacial charge transfer was expected. Futhermore, doping affects the crystallite and particle sizes, the crystal form, and the surface structure; these modifications may be important factors governing the differences in the photoreactivities of doped and undoped TiO_2 (Martin, 1994).

1.4 Research Objectives

The main aim of this research is to develop a photocatalyst which is stable, robust and capable to degrade and mineralize incalcitrant VOCs using visible light or natural sunlight.

The objectives of this research were:

i) to develop an environmental catalyst with excellent photocatalytic activity.
ii) to degrade noxious gases to non toxic gases emitted from industries or other activities using photocatalytic techniques.
iii) to improve the photocatalytic technique by modifying the catalyst.
iv) to characterize the best catalyst using various characterization tools.

1.5 Research Methodology

This research is focus on developing a photocatalyst with high photocatalytic activity to degrade selected volatile organic compounds. The following experimental guidelines were followed in order to achieve the research objectives.

1. The preparation of thin film catalysts using sol-gel technique via the dip coating method.
2. To investigate the effect of doping on the photocatalytic activity of TiO_2. In this research first row transition metal ions are used as dopants and the photoactivity of the catalysts is measured as the rate of VOCs photooxidation.
3. To identify the optimum ratio of metal ions dopants for effective photooxidation of VOCs.
4. To investigate the kinetics of the photocatalytic oxidation of VOCs using the Langmuir-Hinshelwood model.
5. To characterize the structural and optical properties of the best catalyst.

1.6 Scope of Study

This research is focus in developing a photocatalyst with high photocatalytic activities to degrade only hydrocarbon gases. The scope of study include:

i) the introduction of transition metal ions dopants to TiO_2 catalyst.
ii) photodegradation testing of gases under simulated (laboratory scale) condition.
iii) the volatile organic compounds under study were benzene, acetone, toluene, *m*-xylene, and tetrachloroethylene.
v) the photocatalytic studies was conducted under ambient temperature and pressure.

1.7 Significant of Research

In more economically developed and rapidly developing countries recent changes in lifestyles and environmental quality have meant that an increasing number of people are exposed to the contaminants of urban air (Lipfert, 1997). Large quantities of VOCs are emitted into the troposphere from anthropogenic and biogenic sources (Sawyer, 2000) and there is certainly evidence that, especially amongst more vulnerable members of society, these outdoor pollutants may pose a real health risk (Burr, 1995). Immediate action is therefore needed to abate this environmental problem. The findings of this research are meant to help in reducing the problem of air pollution.

CHAPTER II

LITERATURE REVIEW

2.0 Introduction

Titanium dioxide represents one of the most efficient photocatalyst and has great potential in abating environmental problem. However, there are two distinctive disadvantages in using TiO_2 as a photocatalyst. The effective photoexcitation of TiO_2 particles requires the application of light with energy higher than the titania band gap (E_{bg}). For anatase, the E_{bg} value is 3.2 eV and for rutile, 3.02 eV. The absorption threshold, therefore correspond to 380 for anatase and 410 nm for rutile (Hoffman, 1995). Consequently, only the ultraviolet fraction of the solar irradiation (about 5%) is active in the photoexcitation processes using pure TiO_2 solids (Fujishima, 1999).

Another disadvantage of TiO_2 is that the charge carrier recombination occurs within nanoseconds (Rothenberger, 1985). In order for photocatalysis to be productive chemically, electron-hole pair recombination must be suppressed and this can be accomplished by trapping, either the photogenerated electron, the photogenerated hole, or both. In order to enhance interfacial charge-transfer efficiency of TiO_2, the properties of the TiO_2 have been modified by selective surface treatment such as surface chelation (Vrachou, 1989), surface derivatization (Hong, 1987) and metal ion doping (Bahnemann, 1987).

2.1 Transition metal ion doping

Doping implies incorporation of a foreign cation into the catalyst matrix of the parent metal oxide (Karakitsou, 1993). From a chemical point of view, TiO_2 doping is

equivalent to the introduction of defect sites, such as Ti^{3+}, into the semiconductor lattice where the oxidation of Ti^{3+} species is kinetically fast (Fox, 1993). A wide range of metal ions, in particular, transition metal ions, have been used as dopants for TiO_2 and many controversial results are reported. For example, the same dopant used by different authors shows different photocatalytic behaviour towards the same organic compound and the same dopant react differently toward different compounds. A direct comparison and unifying conclusions among results reported for doped samples, therefore, is difficult to make. This variety of results is due to the widely varying experimental conditions, sample preparation and the determination of photoreactivity. Doping titanium dioxide with transition metal ions, however, was envisaged as a good tool to improve photocatalytic properties, principally because an enhancement of the response to the visible region was expected (Litter, 1996) and the enhancement of the photocatalytic activity of TiO_2 by decreasing the recombination rate of e^-h^+ pairs (Moser, 1987).

Metal ion dopants influence the photoreactivity of TiO_2 by acting as electron (or hole) traps and by altering the e^-/h^+ pair recombination rate through the following process.

$$M^{n+} + e_{cb}^- \rightarrow M^{(n-1)+} \quad \text{electron trap}$$

$$M^{n+} + h_{vb}^+ \rightarrow M^{(n+1)+} \quad \text{hole trap}$$

Dopants should act as both electron traps and hole traps to be photoactive. Trapping either electron or hole alone is ineffective because the immobilized charge species quickly recombines with its mobile counterparts (Choi, 1994).

2.1.1 Inhibiting electron-hole recombination

The benefit of introducing dopants into TiO_2 matrix is to improve trapping of electrons and thus inhibit the recombination of e^-h^+ pair by increasing the charge separation (Moser, 1987). However, this statement does not always follows. Co and W-doped TiO_2 showed to be more photoactive than the bare TiO_2 for degradation of methanoic acid and 4-nitrophenol respectively. The behaviour of TiO_2 doped with Fe,

Cu, Cr, Mo, and V, however, was detrimental for both reactions, indicating the enhancement of e^- - h^+ recombination (Di Paola, 2002). Gratzel and Howe (Gratzel, 1990) doped TiO_2 with Fe^{3+} and upon photoirradiation, observed an increased in intensity of the ESR Ti^{3+} signal due to the accumulation of trapped conduction band electrons as Ti^{3+}. This observation showed that doping titania with Fe^{3+} are capable to improve the charge separation of the photoproduced e^-h^+ and inhibit its recombination (Ranjit, 1997). Transition metal such as Cr (Herrmann, 1984), Mo and V (Gratzel, 1990), however, creates acceptor and donor centers that behave as recombination centers for the photogenerated charge carriers. Luo *et al.* (Luo, 1992) reported that doping TiO_2 with molybdenum and vanadium introduced recombination centers in the TiO_2 forbidden band and enhance the surface recombination of the photogenerated electrons and holes.

The same result was also obtained when (Martin, 1994) TiO_2 doped vanadium was used in the photodegradation of 4-chlorophenol. The photooxidation rate of 4-chlorophenol was reduced relative to undoped TiO_2. Vanadium reduced the photoreactivity of TiO_2 by promoting charge-carrier recombination with electron trapping at $>VO_2^+$ site whereas V (IV) impurities in surficial V_2O_5 islands on TiO_2 promote charge-carrier recombination by hole trapping.

Wilke *et al.* (Wilke, 1999) investigated the effect of Cr^{3+} and Mo^{5+} doping on TiO_2 photocatalytic degradation of Rhodamine B. Incorporating these ions into TiO_2 was found to reduce the lifetime of electron and holes from 89.3μs for pure TiO_2 to 30μs in Cr^{3+} and to about 20μs in Mo^{5+} thus decreasing the photocatalytic activity of the photocatalyst.

The production of ammonia from dinitrogen and water vapor at mild conditions of temperature and pressure on Fe^{3+} doped titanium dioxide powders under UV irradiation has been studied (Soria, 1991) in the gas solid regime. A net activity decline was observed. ESR study showed that Fe^{3+} ions are better electron traps than Ti^{4+} ions. Navio et al. (Navio, 1996) prepared specimens of iron doped titania containing different amounts of Fe (0.5-5%) in effort to degrade oxalic acid and EDTA. The photocatalytic efficiency of TiO_2 was reduced and this was attributed to the role of dopant as recombination centers rather than as trap sites for charge transfer at the interface.

2.1.2 Extending the photoresponse

The incorporation of metal ions into titania crystal lattice can significantly extend the absorption by the photocatalysts into visible region. Dopants introduce energy levels into the bandgap, which are responsible for the red shift of the intrinsic absorption edge of TiO_2 and of the enhancement of visible light absorption (Litter, 1996). However, the photoactivity of the prepared doped TiO_2 photocatalyst substantially depends on the dopant ion nature and concentration, besides the method of preparation and the thermal and reductive treatment (Malati, 1984).

Transition metals such as Cr, Mn, V, Fe, have been used to improve the photoresponse of TiO_2 (Hermann, 1984; Ranjit, 1997; Wang, 1999; Wilke, 1999). Among these, Cr seems to be one of the most promising dopant in TiO_2 as it shifts the optical absorption spectrum towards the visible range. However, an excess of chromium leads to the recombination of charge carriers. Cr doping by a chemical method decreased the photoreactivity of TiO_2 under both visible and UV illumination (Borgarello, 1982). No photocatalytic degradation of oxalic acid and EDTA with Fe (III) doped TiO_2 under visible irradiation ($\lambda > 420$ nm) was made but there are some degradation of oxalic acid with catalyst with higher Fe (5wt% Fe/Ti samples) (Navio, 1996). The effect of Cr, Mn and Co-doped TiO_2 was investigated by UV-Vis, FT-IR, near IR and Electron Paramagnetic Resonance (EPR) spectroscopic technique (Dvoranova, 2002). The presence of the doping ions in the titania structure caused significant absorption shift to the visible region compared to pure TiO_2 powder. However, the presence of transition ions in the titania surface has a detrimental effect on the photocatalytic activity.

Recently, rare earth (RE) doped TiO_2 (La^{3+}, Ce^{3+}, Er^{3+}, Pr^{3+}, Gd^{3+}, Na^{3+} and Sm^{3+}) nanoparticles were prepared (Xu, 2002) using the sol-gel method. Their photocatalytic activities were evaluated by nitrite degradation. Results shows that suitable content of doping rare earth in TiO_2 can efficiently extend the light absorption properties to the visible region. RE/TiO_2 samples can enhance the photocatalytic activity to some extend as compared with naked TiO_2. The increase in photoactivity is probably due to the higher absorption, red shifts to a longer wavelength and the increase in the interfacial electron transfer rate. The amount of RE doping, however, was an

important factor affecting photocatalytic activity. The optimum amount of RE doping is ca. 0.5wt% at which each RE/TiO_2 sample shows the most reactivity.

From the above review, it can be concluded that doping can improve the photo-activity of TiO_2 by increasing the rate of e^-h^+ recombination. However, it can also create recombination sites and thus decreases the activity of TiO_2. Although, dopants can improve the photo-response of TiO_2 towards the visible region, it can be detrimental to the photo-activity of the catalyst. A systematic study of metal ion doping, was performed by Choi et al. (Choi, 1994) by measuring their photo-reactivity and the transient charge carrier recombination dynamics. Doping with Fe^{3+}, Mo^{5+}, Ru^{3+}, Os^{3+}, Re^{5+}, V^{4+} and Rh^{3+} significantly increases the photo-reactivity for the oxidation of $CHCl_3$ and reduction of CCl_4 while Co^{3+} and Al^{3+} doping decreases the photo-reactivity. Choi concluded that the photo-reactivity of doped TiO_2 appears to be a complex funtion of the dopant concentration, the energy level of dopants with the TiO_2 lattice, their d electronic configuration, the distribution of dopants, the electron donor concentration and the light intensity.

Radecka *et al.* (Radecka, 2002) studied the structural and optical properties of titanium dioxide doped with Cr. The increase in Cr concentration shifts the entire absorption spectrum towards the visible range. Acceptor impurities, such as Cr, create the allowed states in the forbidden band gap of TiO_2. The Cr^{3+}/d^3 energy levels are localized within the optical band gap of TiO_2. Substitution of Ti by d^n metallic ions into the lattice of stable TiO_2 can induce photoactive transitions in the visible region between chromium ions and conduction band.

Palmisano *et al.* (Palmisano, 1988) studied the photoreduction of dinitrogen to ammonia in a gas-solid regime and the photodegradation of phenol in an aqueous liquid-solids regime using a series of chromic-ions and iron-ions-containing titania specimens. For the photoreduction reaction it was found that the presence of the dopants is essential for the occurrence of the photoreactivity, the iron-ions-containing specimens being more effective than those containing chromic ions. For the photooxidation reaction, the presence of dopants instead, the photoreactivity of titania is not affected or, in some cases detrimentally affected. The two contrasting behaviours are explained by taking into account the differences in the gas-solid and liquid-solid interfaces.

CHAPTER III

3.0 EXPERIMENTAL

3.1 Chemicals and Reagents

All the chemicals used were reagent-grade. For catalysts preparation, absolute ethanol (99.7%) was purchased from Hayman Limited, polyethylene glygol (PEG) (MW = 200) and diethanolamine (DEA) was from Merck-Schuchandt and titanium tetraisopropoxide ($Ti(iso)_4$) was purchased from Aldrich. All the transition metal ions precursors used as dopants are acetates except for iron nitrate obtained from GCE Laboratory Chemicals. The volatile organic compounds used in the photocatalytic degradation test are benzene, toluene, acetone and *m*-xylene purchased from Wako Pure Chemical Industries, LTD, and tetrachloroethylene (TeCE) from Kanto Chemical Co. LTD. All chemicals were used as received.

3.2 Catalyst Preparation

The TiO_2 solution was prepared by the sol-gel technique. 6 g PEG was added to 600 mL ethanol in a cornical flask and the solution was stirred continuously. When all PEG has dissolved, 31.8 g DEA and 85.2 g $Ti(iso)_4$ was added simultaneously to the solution. Finally 5.4 mL H_2O was added. The sol-gel solution prepared was clear and colorless. The sol-gel was then used to prepare the doped TiO_2. For each metal ion doped TiO_2, five (5) series of ratios (mole ratio) were prepared; 1:0.01, 1:0.005, 1:0.001, 1:0.0005 and 1: 0.0003. For Ag^+ however, only 4 ratios, 1:0.005, 1:0.001, 1:0.003 and 1:0.0005 were prepared due to the difficulty in dissolving silver acetate in TiO_2 sol. A calculated amount of the metal ions was added to the TiO_2 sol and stirred

until dissolved. The product solution are clear and where coloured solution was obtained, the colour will depend on the kind of metal ion present.

The preparation of the thin film utilized the dip coating method (Brinker, 1991). The sol was coated on pyrex glass hollow cylinders 14.5 cm long with internal diameter 3.4 cm. The glasses were pre-washed with alkaline solution prior to the coating process. The dipping and drying processes were repeated 5 times. The gel coatings were then dried at 81°C for 1 hr in the oven before calcination. The calcination temperature was elevated slowly (2 °C/min) to 600 °C and kept for 1 hr. All the thin films prepared are clear and colourless.

3.3 Photoactivity Measurements

All degradation processes of the organic compounds were carried out in a glass reactor with a total volume of about 1000 mL. A basic experimental set up in this research is shown in Fig. 3.1. Illumination was provided by a light source from a Toshiba 6 W black light lamp with a maximum at 354 nm. The amount of VOCs degraded in all the photodegradation tests were stated as percentage degraded. Prior to the photodegradation tests, calibration graphs for all VOCs under study were obtained (Appendix 1).

In a typical experiment, the reactor was first vacuumed to remove any residual contaminants. The desired amount of organic compound was injected through a sample port into the reactor, where evaporation occurred. Air was introduced inside the reactor by opening one of the reactor taps. The air stream contaminated with the organic compound was passed through the reactor until gas-solid adsorption reached equilibrium (typically 30-45 minutes depending on the nature and concentration of the VOC) as indicated by the identical VOC concentrations analyzed regularly before illumination. When this was achieved the UV illumination was turned on. Samples were taken at regular time intervals and analyzed by GC (Shimadzu GC-17A) operating with a FID and a fused silica capillary column.

The photodegradation of benzene was first carried out to identify the catalysts with the optimum ratio of dopants. These catalysts increased the activity of TiO_2 by increasing the photodegradation rate of benzene and giving the highest percentage of benzene conversion. The catalysts with the optimum ratio of dopants were then used to degrade other VOCs (toluene, acetone, xylene and tetrachloroethylene). The best dopant for each organic compound was further used in the kinetics study.

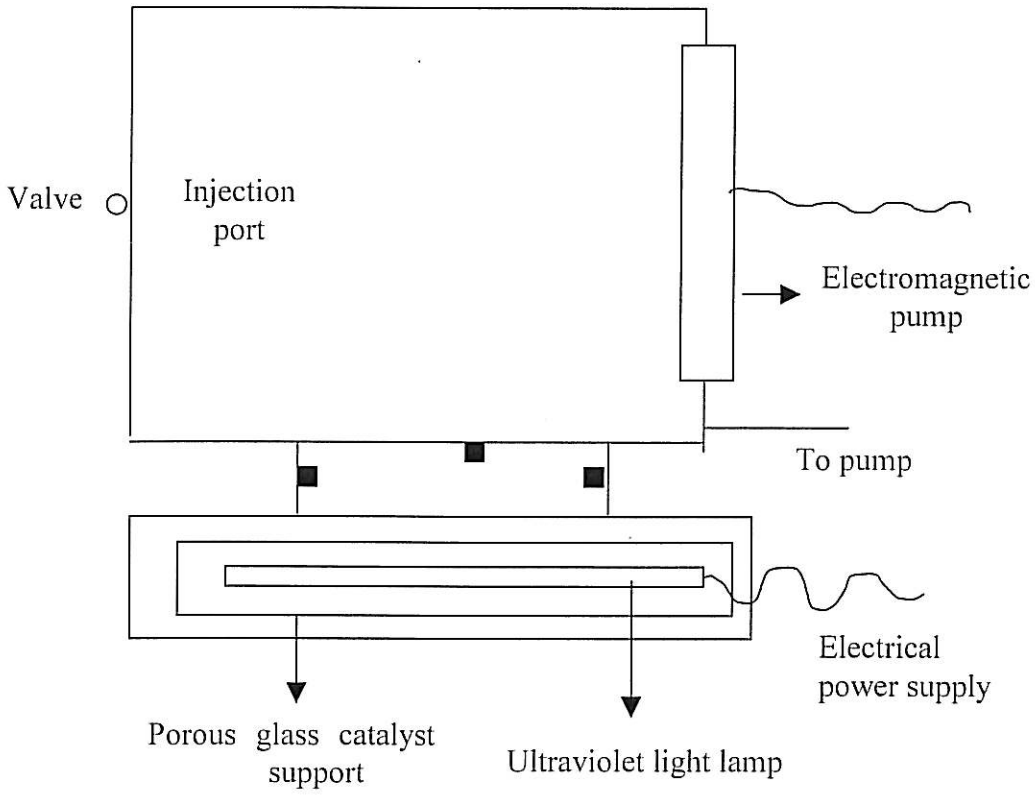

Figure 3.1: Photocatalysis Reactor Scheme

3.3.1 Kinetics Study

The procedure used in the kinetics study of the photodegradation reaction is the same as in the photoactivity measurements. Five (5) different concentrations (2μ. 3μ, 4μ, 6μ and 8μ) of each organic compound were degraded with a total illumination time of 15 to 20 minutes, analyzing each sample after every 3 to 5 minutes irradiation time. The initial rate of each reaction was calculated using the first 15 minutes of the

photodegradation data. The reciprocal value of the initial rate (1/r) was then plotted against the reciprocal values of the organic compound initial concentration ($1/C_o$). If the reaction follows the L-H model the plot of will exhibits a linear relationship. The intercept is k^{-1} and the slope is $(kK)^{-1}$. k is the rate constant related to the limiting rate of reaction at maximum coverage and K is the adsorption constant and reflects the proportion of solute molecules which adhere to the catalyst surface.

The kinetics study of benzene and acetone was conducted using undoped and Fe^{3+} and Ag^{+} doped TiO_2. While for toluene kinetic study, undoped and Zn^{2+} doped TiO_2 was used as catalyst. Kinetic study for TeCE photodegradation was conducted using only undoped TiO_2 as dopants has no affect on TeCE degradation.

3.4 Characterization Tools

In this research, the structural, chemical and optical properties of the catalysts were investigated. Characterization techniques such as Ellipsometer (film thickness and refractive index), X-ray Diffraction (film crystallinity and crystal phase), X-ray Photoelectron Spectroscopy (film composition, oxidation state of elements), Scanning Electron Microscope/Electron Dispersive X-ray Analysis (film morphology and elemental analysis), UV-Vis spectroscopy (absorption and transmittance and band gap), and Photoluminescence Spectrophotometer (transition energy) were employed.

The ellipsometer used to determined the film thickness and refractive index was a single wavelength (623.4 nm) Gaertner model L117. The data obtained from the ellipsometry measurements were processed using "*bbc ellip*" software analysis program.

The crystallinity of the thin films was determined by X-ray diffraction (XRD) analysis. The X-ray diffractogram was obtained using the thin film samples. The XRD instrument was RAX01 of Rigakudenki Co. equipped with Cu-K_α (λ = 1.54056 Å) radiation. The operating mode of the diffractometer is 40.0 KV, 30.0 mA and with a scanning speed of 1.0 deg/min.

The X-ray photoelectron Spectroscopy (XPS) was used to detect the chemical species on the catalyst surface. Measurements were carried out using a Kratos XSAM HS surface analysis spectrometer with MgK_{α} X-ray source (1253.6 eV). A 10 mA current and 14 kV energy source were employed to record the spectrum. Survey scans in the range of 10-1100 eV were recorded at a pass energy of 160 eV with a step size of 1 eV $step^{-1}$ and a sweep time at 300 second $sweep^{-1}$. Narrow scan were obtained for C (1s), O (1s), and Ti (1s) regions at 20 eV pass energy, 0.1 eV $step^{-1}$ and sweep time at 59.898 second $sweep^{-1}$.

Surface morphology was characterized using Scanning Electron Microscope (SEM) model Phillip XL40 interfaced with a PC through Phillip XL software (version 5.01). Samples were bombarded using an electron gun with a tungsten filament under a 25 kV resolution. The Electron Dispersive X-ray Analysis (EDAX), model Ametek, version 3.32 XL, is linked to the SEM and uses X-rays to identify trace amounts of elements on the surface of the scanned test specimen.

UV-Vis Spectroscopy was used to obtain absorbance, transmittance and reflectance data for the thin films. These data was used to determine the band gap values of the pure and doped thin films. The optical spectra were recorded using a UV-VIS-NIR Shimadzu UV-3101PC Spectrometer in the wavelength range 300 – 800 nm.

CHAPTER IV

4.0 RESULTS AND DISCUSSIONS

4.1 Optimum Ratios

The photooxidation of benzene using all ratios of metal ions doped catalyst showed an interesting trend where an optimum ratio was obtained for all metal ions. Except for Co^{2+} and Zn^{2+}, which have an optimum ratio 1:0.001, Ag^{+} 1:0.003, all the other metal ions showed an optimum of 1:0.0005 (Figure 4.1). The bar chart shows the time taken for each metal ion doped catalyst to degrade ~90% of benzene. The best ratio of metal ions doped TiO_2 increased the rate of benzene photooxidation. This optimum concentration of dopants can be related to the charge transfer process involved in the photocatalytic mechanisms. Once excitation occurs in the semiconductor, the created electron and hole pair can undergo charge transfer to adsorbed species on the semiconductor surface. The existence of dopant oprimum ratio was also observed by other researches (Schrauzer (1977), Choi (1994), Palmisano (1988) and Litter and Navio (1996).

The existence of the optimum value can also be associated with the amount of active sites on TiO_2. When the concentration of dopants is low, the density of reactive sites at the catalyst surface would decrease. Only a small amount of photocatalytic reaction can occur on the catalyst surface. These active sites however will be easily blocked if the amount of dopants is too high or above the optimum value. The blocking process will reduce the probability of further charge transferring process and consequently decreasing the amount of photocatalytic reaction.

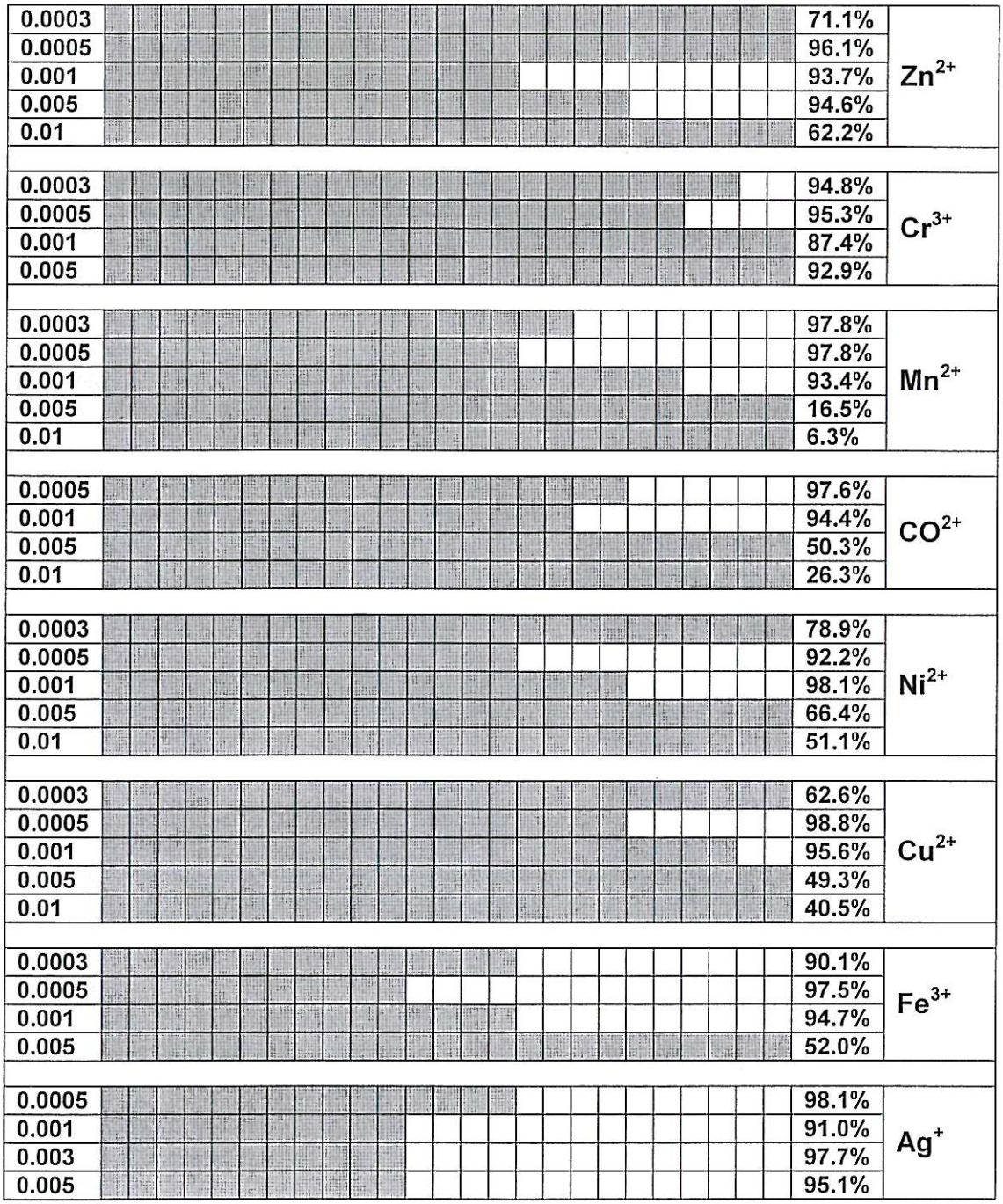

Figure 4.1: Bar chart showing the amount of benzene degraded using different ratios of doped TiO_2. Note: Each column represents a 5 minutes time scale.

4.2. Effect of Wavelength

Table 4.1 shows the effect of different wavelength light source on the photodegradation of benzene using pure TiO_2. For both UV lamps (254 nm and 354 nm) the data represents the time taken for 90% of benzene to degrade. However, in the fluorescence light column, the value in the bracket shows the amount of benzene degraded in 120 minutes.

Table 4.1: Photodegradation of benzene using 254 nm, 354 nm, and fluorescence light source.

Catalyst	Time (minutes)		
	254 nm (90%)	354 nm (90%)	Fluorescence
TiO_2	**31**	**55**	**120 (11%)**
Fe^{3+}	**22**	**45**	**120 (21%)**
Ag^{+}	**21**	**45**	**120 (17%)**
Zn^{2+}	**29**	**66**	**120 (12%)**
Mn^{2+}	31	72	120 (10%)
Cu^{2+}	33	88	120 (10%)
Co^{2+}	60	82	120 (5%)
Cr^{3+}	60	98	120 (9%)
Ni^{2+}	40	73	120 (3%)

The rate of benzene degradation was much higher using shorter wavelength light source. Although the amount of benzene degraded was low using fluorescence lamp, it was substantial enough to show that photodegradation using fluorescence lamp can be achieved. Electron and hole are generated through the absorption of photon with energy equal or higher than the band gap energy. It is known that energy is proportional to the number of photons ($E = h\nu$). Therefore the higher energy the light is the more number of photons it has. Thus more electron and hole pairs will be produced and this will increased the degradation rate.

4.3 Photodegradation of VOCs Using Doped TiO_2 Thin Films.

All experiments were carried out using optimum ratio of metal ions irradiated with UV light source for two (2) hours except for acetone where total illumination time was one (1) hour. Gas samples were analyzed periodically using GC.

4.3.1 Benzene

Table 4.2 shows the percentage degradation of benzene against time of irradiation in minutes for high and low concentration of benzene respectively, using TiO_2 and doped TiO_2. The concentration of benzene used varies from 630-800 ppm for high and 280-430 ppm for low concentration of benzene.

Table 4.2: Rate of benzene degradation, (H and L – high and low concentration respectively). Time taken for 90% of benzene to degrade.

Catalyst	Time (minutes)	
	(L)	(H)
TiO_2	**30**	**55**
Cr^{3+}	68	98
Fe^{3+}	**26**	**45**
Ni^{2+}	44	73
Cu^{2+}	38	88
Co^{2+}	64	82
Zn^{2+}	34	72
Mn^{2+}	35	66
Ag^{+}	**32**	**45**

Fe^{3+} and Ag^{+} showed a significant increased in TiO_2 photoactivity with high concentration of C_6H_6, where 90% of C_6H_6 was degraded in 45 minutes for both metal ions. The same amount of benzene was degraded in 55 minutes when undoped TiO_2 was

used during the oxidation process. The other metal ions gave a negative effect in the photooxidation of benzene. When the concentration of benzene was reduced, TiO_2 doped Fe^{3+} was observed to degrade 90% of C_6H_6 in 26 minutes as compare to the undoped TiO_2 (30 minutes). Ag^+ however is detrimental as with the other metal ion dopants.

The presence of Fe^{3+} has essentially increases the photooxidation rate of benzene both in low and high concentration. In gas-phase photocatalysis, the role of dopant is to inhibit the recombination of holes and electrons by acting as electron and hole trap. Fe^{3+} increased the photodegradation of benzene by acting as electron and hole trap, thus increased the lifetime of both species.

The addition of Ag^+ was beneficial due to the high efficiency of Ag^+ as electron scavenger. It was suggested that AgO photodeposited onto TiO_2 improved charge separation and oxygen reduction efficiency. Kim (1996) attributed the inhibition caused by silver ions in the photocatalytic and photoelectrocatalytic degradation of HCOOH on TiO_2 thin films to the formation of Ag^0 deposited on the catalyst surface.

The addition of Mn^{2+}, Co^{2+}, Ni^{2+}, Cu^{2+} and Zn^{2+} to TiO_2 gave a detrimental affect to the photocatalytic reaction of benzene. Palmisano (1988), Dvoranova (2002) and Di Paola (2002) also observed the same detrimental effect of these cations in the photodegradation of aqueous system. The separation of the photogenerated electron and hole is not effective in these doped catalysts. Therefore the recombination rate of electron and hole increased thus reduced the photodegradation of benzene.

4.3.2. Toluene

The concentration of toluene used in the study varies from 480-525 ppm for high and 270-320 ppm for low concentration. Table 4.3 shows the photoactivity of TiO_2 and doped TiO_2 on the photooxidation of toluene. Fe^{3+}, which gives a positive effect on C_6H_6 degradation, however is detrimental to toluene degradation in both high and low concentration. Zn^{2+}, however, increased the photooxidation of toluene with low and

high concentration of toluene compared to undoped TiO_2. The other metal ions were deleterious to toluene photooxidation.

Table 4.3: Rate of toluene degradation, (H and L – high and low concentration respectively).

Catalyst	Time (minutes)	
	(L) 90%	(H) **
TiO_2	**54**	**175**
Cr^{3+}	110	186
Fe^{3+}	63	*-
Ni^{2+}	90	194
Cu^{2+}	99	174
Co^{2+}	109	186
Zn^{2+}	**43**	**86**
Mn^{2+}	103	232
Ag^{+}	72	195

*Saturation occurred at 120 minutes with 37% of toluene oxidized
**Data obtained by extrapolating the graphs backwards to the 100% line.

90% of toluene was degraded in 43 minutes as compared with undoped TiO_2 (54 minutes) in low concentration of toluene. With high concentration of toluene, the Zn^{2+} doped TiO_2 catalyst showed high photoreactivity, where about 90% of toluene was degraded in 86 minutes. However, the same amount of toluene was degraded in 175 minutes with the undoped catalyst. Fe^{3+} doped TiO_2 was detrimental to toluene oxidation where only about 40% of toluene was oxidized. This catalyst showed a saturation point at 125 minutes reaction time.

When calcined at 600°C, Zn^{2+} would be decomposed into ZnO. The oxide dispersed on the TiO_2 surface can involve some charge transfer with TiO_2 during illumination due to the difference in the energy band position. As the valence band of TiO_2 is lower than that of ZnO (Yuan, 2002), the generated holes can be transferred

from TiO_2 to ZnO. This can promote the charge separation of the generated carriers. Interfacial charge transfer process can also be promoted, as more of the Zn ions were distributed near the surface because of the larger Zn^{2+} size compare to Ti^{4+}. Hole detrapping will be easier and this will thus improve the photocatalytic activity of TiO_2 as more hydroxyl radical will be formed.

The detrimental effect of Cr^{3+}, Co^{2+}, Ni^{2+} and Mn^{2+} can be attributed to the fact that these cations creates acceptor and donor surface sites, acting as a recombination center. Furthermore, as the sizes of these cations are smaller or similar to Ti^{4+}, most of these cations will be found deeper in the host catalyst. This will reduced the efficiency of charge transfer process near the catalyst surface, increased the probability of electron-hole recombination and thus reduced the photocatalytic activity of TiO_2.

4.3.3 *m*-Xylene

The concentration of *m*- xylene used in this study varies between 200-280 ppm for low and 310-430 ppm for high concentration. Tables 4.4 shows the amount of *m*-xylene oxidized after 120 minutes illumination time with undoped and doped TiO_2. All metal ions giving a detrimental affect on the degradation of benzene and toluene gives the same effect on xylene. Only Zn^{2+} increased the activity of TiO_2 in *m*-xylene photooxidation.

With low concentration of *m*-xylene, 97 % of the VOC was degraded in 120 minutes when Zn^{2+} doped TiO_2 was used during the photocatalytic process. The amount degraded when undoped TiO_2 was used was 90 %. This show a 7% increased in the amount of *m*-xylene degraded. With high *m*- xylene concentration 62 % of *m*-xylene was degraded with Zn^{2+} doped TiO_2 as compared to 55 % using undoped catalyst. The same percentage increased of *m*-xylene photooxidation. All the other dopants, however, reduced the photoactivity of TiO_2.

Table 4.4: Amount of *m*-xylene degraded after 120 minutes illumination time (H and L – high and low concentration respectively).

Catalyst	% Degraded	
	(L)	(H)
TiO_2	**90**	**55**
Cr^{3+}	76	44
Fe^{3+}	46	35
Ni^{2+}	82	**45**
Cu^{2+}	**90**	48
Co^{2+}	73	42
Zn^{2+}	**97**	**62**
Mn^{2+}	89	**45**
Ag^{+}	87	53

All metal ions that gave a detrimental affect on the degradation of benzene and toluene gave the same effect with *m*-xylene. Only Zn^{2+} increased the activity of TiO_2 in *m*-xylene photooxidation, a similar observation made in the photooxidation of toluene. The same explanation for toluene photodegradation could be used in describing the high activity of Zn^{2+} doped TiO_2 in *m*-xylene photodegradation. Zn^{2+} being a good hole trap, could promote the participation of the photogenerated electron in *m*-xylene oxidation. However, because *m*-xylene contained two methyl groups, the participation of the electrons could be hindered. This will lead to a lower *m*-xylene conversion.

4.3.4 Acetone

The concentration of acetone used in the study was in the range of 740-890 ppm and 380-480 ppm for high and low concentration respectively. Table 4.5 shows the amount of acetone degraded.

TiO_2 exhibited a high photocatalytic activity in acetone photodegradation for both concentrations where almost 100% of acetone was degraded. All doped catalysts gave a detrimental effect on the photodegradation of low acetone concentration. However, with higher acetone concentration, the activity of TiO_2 increased slightly with the addition of Fe^{3+} and Ag^{+} following the trend of benzene degradation. 90% of acetone was degraded in 23 and 27 minutes when Fe^{3+} and Ag^{+} doped TiO_2 respectively, was used in the photooxidation process of high concentration of acetone while 29 minutes was taken to degrade the same amount of acetone using undoped catalyst. Zn^{2+} however has a negative effect.

Table 4.5: Rate of acetone degradation, (H and L – high and low concentration respectively). Time taken for 90% of acetone to degrade

Catalyst	Time (minutes)	
	(L) 90%	(H) 90%
TiO_2	**19**	**29**
Cr^{3+}	39	57
Fe^{3+}	21	**23**
Ni^{2+}	27	42
Cu^{2+}	26	32
Co^{2+}	43	62
Zn^{2+}	29	39
Mn^{2+}	28	38
Ag^{+}	21	**27**

4.3.5 TeCE

The initial concentration of TeCE used in the study varies from 650 – 780 ppm for high concentration of TeCE and 250-380 ppm for low concentration. Table 4.6

shows the photooxidation of TeCE using doped and undoped TiO_2. High photooxidation of TeCE using both pure and doped catalyst was observed. Dibble and Raupp (1990), Nimlos (1993) and Jacoby (1995) also made the same observations with the photooxidation of trichloroethylene (TCE).

Table 4.6: Amount of TeCE degraded after 3 minutes of illumination time (H and L – high and low concentration respectively)

Catalyst	% Degraded	
	(L)	(H)
TiO_2	**98.25**	**98.25**
Cr^{3+}	93.19	71.33
Fe^{3+}	92.43	94.97
Ni^{2+}	93.55	89.89
Cu^{2+}	93.29	90.80
Co^{2+}	76.93	71.37
Zn^{2+}	85.41	61.56
Mn^{2+}	90.10	79.34
Ag^{+}	93.51	91.90

Table 4.6 shows the amount of TeCE oxidized in 3 minutes when doped and undoped TiO_2 was used in the photooxidation process. The initial rate of TeCE photocatalytic oxidation was observed to be higher than benzene, toluene, acetone and *m*-xylene oxidation using all dopants. About 90 % of TeCE was oxidized only within 5 minutes of reaction for both TeCE concentrations. For low concentration of TeCE, the amount of TeCE oxidized after 3 minutes of photoreaction is 98.96 % using undoped TiO_2. The other metal ions show lower initial rate of TeCE degradation. For higher TeCE concentration 98.25% of TeCE was degraded using pure TiO_2. All the other doped catalyst showed a comparable or lower reactivity to pure catalyst. However if the illumination time is prolonged to 6 minutes, almost 98 % of TeCE was degraded using all dopants for both concentrations.

The introductions of dopants into TiO_2 matrix did not affect the photoactivity of TiO_2 in TeCE photooxidation. Although the amount of TeCE degraded was lower using doped catalyst, with a longer reaction time (~ 5 minutes) the amount of TeCE degraded for all catalyst reached almost 100%. The high photocatalytic oxidation of TeCE therefore could be due primarily to the chlorine atom from the hydrocarbon and not to the dopant.

In the photooxidation using TiO_2, it is well established that hydroxyl radicals (HO•) are the major reactive species for the oxidation of organic compounds. In this study the reaction rates of TeCE photocatalytic oxidation was observed to be far higher than the non-chlorinated hydrocarbons. These high photooxidation rates imply that a different mechanism may be occurring in the oxidation process. Dibble suggested that chlorine radicals could be initiating TCE oxidation in the gas phase and proceeds through a chain mechanism. As the structures of both VOCs are similar, chlorine radical could also be responsible for the higher photooxidation of TeCE. The chlorine radical can be produced during TeCE photodegradation by the reaction of h^+ or hydroxyl radical with TeCE. The chlorine radical can then react with other TeCE molecules, thus creating a chain reaction.

4.4 Kinetics study

The catalysts used for the kinetics study are the previously prepared TiO_2 doped catalysts with the optimum mole ratio - Fe^{3+} (1:0.0005), Ag^+ (1:0.003) and Zn^{2+} (1:0.001). The Fe^{3+} and Ag^+ catalysts were used in the kinetics study of benzene and acetone while Zn^{2+} for toluene kinetics study. Due to the lower conversion (destruction) rate observed for *m*-xylene with undoped TiO_2 and TiO_2 doped Zn^{2+}, further kinetic refinement were not conducted in this study.

In this research all the kinetics data were obtained from the initial rate of the photodegradation reaction and all were well described by the L-H rate forms. Table 4.7 summarizes the information on the kinetics of photodegradation for all organic compounds under study.

Table 4.7: Langmuir-Hinshelwood parameters obtained in the photocatalytic destruction of volatile organic compounds

(a) Benzene

Catalyst	k (ppm/min)	K (ppm^{-1})
TiO_2	47.17	5.81×10^{-4}
Fe^{3+}	25.32	1.13×10^{-3}
Ag^{+}	13.59	5.1×10^{-3}

(b) Toluene

Catalyst	k (ppm/min)	K (ppm^{-1})
TiO_2	35.09	7.37×10^{-4}
Zn^{2+}	18.76	1.91×10^{-3}

(c) Acetone

Catalyst	k (ppm/min)	K (ppm^{-1})
TiO_2	125.00	8.07×10^{-4}
Fe^{3+}	54.64	3.49×10^{-3}
Ag^{+}	94.34	1.63×10^{-3}

(d) Tetrachloroethylene

Catalyst	k (ppm/min)	K (ppm^{-1})
TiO_2	1.0×10^{4}	2.28×10^{-4}

It is interesting to note that the degradation rate is dependent on K and k; therefore, a higher adsorption constant does not always result in a higher degradation rate. Data from Table 4.7(c) show that the adsorption of acetone on to the surface catalyst was high with TiO_2 doped Fe^{3+} followed by Ag^{+}. Acetone is least adsorbed on undoped TiO_2 surface as indicated by the K values. (K values were 5.4×10^{-3}, 3.5×10^{-3} and 6.92×10^{-4} for Fe^{3+}, Ag^{+} and TiO_2 respectively) However the limiting rates described by the values of k follow the opposite order. Thus although acetone is much more strongly adsorbed on TiO_2 doped Fe^{3+} surface, the destruction rate is not as high

as the undoped TiO_2. TeCE, however shows the highest value for rate constant and the least adsorption constant among the organic compound studied.

The effect of different dopants on the photodegradation rate of TeCE was not carried out. TiO_2 showed a very outstanding photocatalytic activity with TeCE where more than 90% of TeCE was degraded within 5 minutes illumination time with TiO_2.

4.5 Mechanism

Intermediates and products formed during photocatalytic oxidation could be used to determine the photocatalytic mechanism involved in the oxidation process. Table 4.8 shows the intermediates and products formed during the photocatalytic oxidation of VOCs under studied, analyzed using GC-MS.

Table 4.8: Intermediates and products formed during VOCs photocatalytic Oxidation using undoped and doped TiO_2 thin films calcined at 600°C for 1 hour.

VOCs	Intermediated/Products	Catalyst
Benzene	CO_2, H_2O	TiO_2, TiO_2/Fe^{3+}, TiO_2/Ag^+
Toluene	CO_2, H_2O, benzaldehyde (traces)	TiO_2/Zn^{2+}
	CO_2, H_2O, benzaldehyde (traces), benzyl alcohol (traces), benzoic acid	TiO_2
Acetone	CO_2, H_2O	TiO_2, TiO_2/Fe^{3+}, TiO_2/Ag^+
m-xylene	CO_2, H_2O	TiO_2, TiO_2/Zn^{2+}
TeCE	CO, CO_2, Cl_2, CCl_4 (traces), $COCl_2$ (traces), C_2Cl_3OOH (traces)	TiO_2

From Table 4.8, it can be assumed that in benzene photooxidation the hole trapped in Fe^{4+} will be released and consequently react with hydroxyl ion producing hydroxyl radical. This hydroxyl radical will then react with benzene. In Ag^+ doped

TiO_2, the Ag^+ can act as a good electron scavenger. Larger amount of photogenerated holes can reach the interfacial region of Ag^+ doped TiO_2 film producing higher densities of reactive radicals such as OH•. Therefore it is obvious that in benzene photocatalytic oxidation, the hydroxyl radical is the primary reactant.

In this study carbon dioxide and water were the only products formed in benzene photocatalytic oxidation. This observation was similar to the reports made by previous researchers. The possible benzene photocatalytic oxidation pathway proposed in this study is depicted in Figure 4.2. It was difficult to completely and precisely identify the exact mechanisms of benzene photodecomposition as no intermediates were detected.

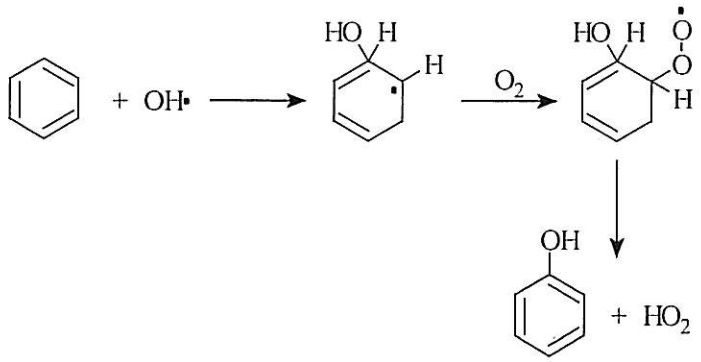

Figure 4.2: A proposed degradation mechanism for the photocatalytic oxidation of gaseous benzene by UV/TiO_2 process vis the hydroxyl radical.

The hydroxyl radical (OH•) attack was believed to be the predominant mechanism for benzene degradation. OH• radical addition to benzene yielded a cyclohexadienyl radical (Reaction a). Subsequent addition of oxygen to this radical and the elimination of the radical HO_2• produced phenol by analogy with what has been determined in water (d'Hennezel, 1998). The photocatalytic process together with OH• and water was involved in the ring opening reactions that result in the final production of CO_2 and H_2O.

The hydroxyl radical is also the primary mechanism for toluene photocatalytic oxidation. However because Zn^{2+} can act as an efficient hole trap for toluene and *m*-xylene photocatalytic oxidation, the photogenerated electron could also be considered to

react directly with toluene and *m*-xylene. The participation of h^+ in toluene photocatalytic oxidation, however, could not be ruled out. Based on the intermediates and products formed during photodegradation of toluene using TiO_2 the possible photocatalytic oxidation pathway for toluene is given below. The photocatalytic oxidation of *m*-xylene was suggested to follow the same reaction pathway as toluene because both VOCs have similar structure.

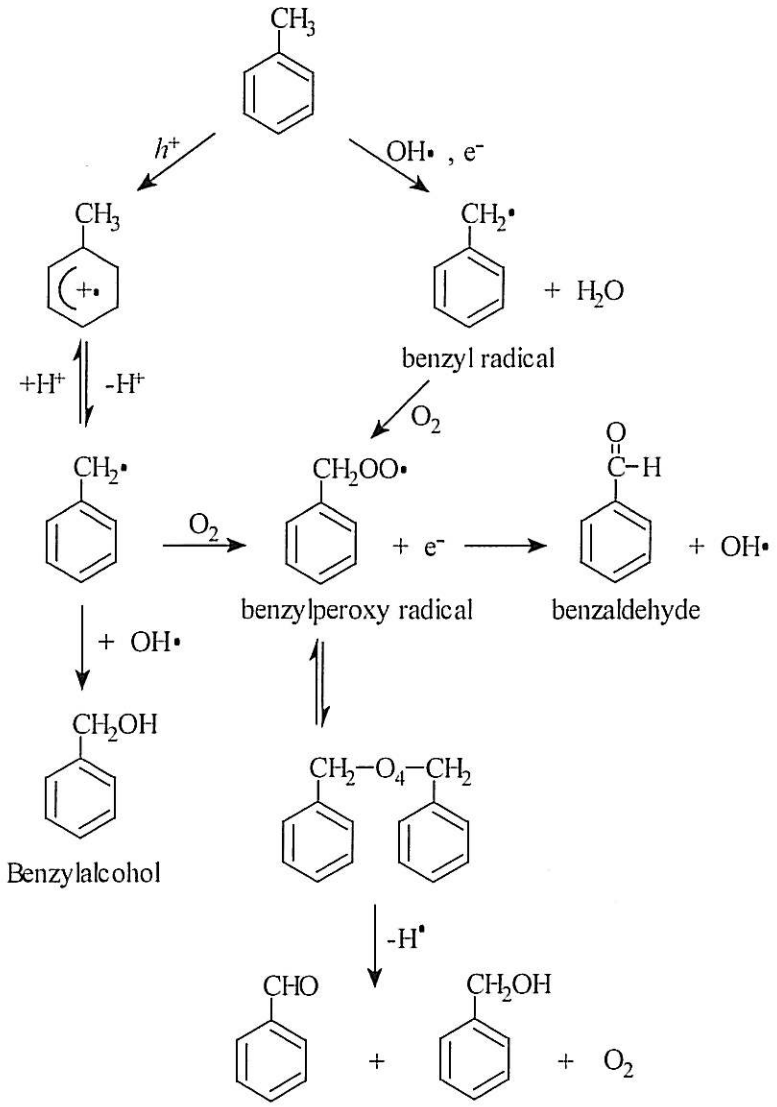

Figure 4.3: A proposed mechanism for toluene photocatalytic oxidation by hole and hydroxyl radical.

In the acetone photocatalytic oxidation no reaction intermediates were detected. This was consistent with most studies concerning the photocatalytic oxidation of acetone. Figure 4.4 depicted the mechanism of direct photocatalytic conversion of acetone to CO_2 and water. However, prior studies by Bickley *et al.* (1973) on rutile TiO_2 powder at much higher partial pressures have reported trace formaldehyde (H_2CO) formation with CO_2 and water as the major and final products. Thus, low concentration of acetone in this study appears to be cleanly converted to CO_2 and water by means of heterogeneous photocatalysis over TiO_2. In the present study, if formaldehyde was formed, it could not be detected by the gas chromatographic analyses, as its concentration is low. However, the possible formation of formaldehyde in acetone degradation could not be rule out. It was also believed that acetone adsorbs on TiO_2 powder to form a physisorbed, H-bonded species (Xu, 2001). The same initial process could be employed to TiO_2 thin film as the first step in acetone photocatalytic oxidation.

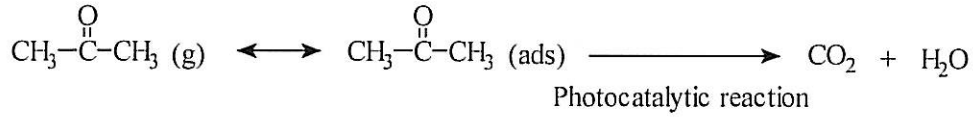

Figure 4.4: A proposed mechanism for direct photocatalytic oxidation of acetone oxidation on TiO_2

The photocatalytic oxidation of TeCE was observed to be much higher than the photocatalytic oxidation of other VOCs under studied and dopants did not affect the photodegradation rate. A different reaction mechanism therefore could be involved in the photocatalytic oxidation of TeCE. In the mechanism for trichloroethylene (TCE) homogeneous photocatalytic oxidation reaction Sanhueza *et al.* (1976) proposed a chain reaction mechanism that involved Cl• atoms attacking TCE to initiate the oxidation reaction. The Cl• atoms required for the TCE photooxidation reaction were produced by an initiation reaction involving TCE. A similar initial reaction can proceed in TeCE photocatalytic oxidation. In the presence of water vapor, hydroxyl radicals will attack the TeCE molecules forming Cl radicals. The Cl radicals then attack more TeCE molecules forming intermediates and products, thus creating a chain reaction process.

The same chain reaction mechanism was also proposed for the photocatalytic oxidation of trichloroethylene (TCE) (Nimlos, 1993).

A possible source for the Cl atoms is the reaction of TeCE with photocatalytically produced hydroxyl radicals.

$CCl_2=CCl_2 + OH\bullet \rightarrow \bullet CCl_2CCl_2OH$ (3.1)

$\bullet CCl_2CCl_2OH + O_2 \rightarrow \bullet OOCCl_2CCl_2OH$ (3.2)

$2(\bullet OOCCl_2CCl_2OH) \rightarrow 2(\bullet OCCl_2CCl_2OH) + O_2$ (3.3)

$\bullet OCCl_2CCl_2OH \rightarrow CCl_2OHCClO + Cl\bullet$ (3.4)

It is plausible that Reactions 3.1-3.4 could occur on the TiO_2 surface during the photocatalytic oxidation of TeCE as an initiation step to the chain reaction. The Cl• then adds to the carbon atom of TeCE. The carbon centered, radicals subsequently react with oxygen to form peroxy radicals. These species are converted to alkoxy radicals by reaction with a second peroxy radical.

$CCl_2=CCl_2 + Cl\bullet \rightarrow CCl_3\ CCl_2\bullet$ (3.5)

$CCl_3CCl_2\bullet + O_2 \rightarrow CCl_3CCl_2OO\bullet$ (3.6)

$2(CCl_3CCl_2OO\bullet) \rightarrow 2(CCl_3CCl_2O\bullet) + O_2$ (3.7)

Based on the intermediates (phosgene, CCl_4) formed during photodegradation of TeCE, the chlorinated ethoxy radicals may undergo two feasible routes: one is the C-C bond scission yielding phosgene and trichloromethyl radicals (Equation 3.8) which latter react with Cl radicals forming CCl_4 and another is the production of trichloroacetylchloride and Cl atom (Equation 3.9).

$CCl_3CCl_2O\bullet \rightarrow CCl_3\bullet + CCl_2O$ (3.8)

$CCl_3CCl_2O\bullet \rightarrow CCl_3CClO + Cl\bullet$ (3.9)

$2Cl\bullet \rightarrow Cl_2$ (3.10)

Trichloroacetylchloride is adsorbed on the TiO_2 surface and further reacts with water adsorbed onto the surface of TiO_2:

$$CCl_3CClO + H_2O \rightarrow CCl_3COOH + HCl \quad (4.38)$$

HCl was not observed in this study as the amount of water is low and no additional water was added to the system. HCl could also be adsorbed on the catalyst surface. However, traces of dichloroacetic acid were detected from the GC-MS analysis. Phosgene (CCl_2O) can be removed by passing the product gas stream through water in which HCl and CO_2 are produced by hydrolysis (Morisson, 1987) or by water molecules adsorbed onto the TiO_2 surface (Yamazaki-Nishida, 1996).

4.6 Characterization

Characterization was conducted on all catalysts samples with the optimum ratio except for elemental analysis using XPS, which was conducted on undoped TiO_2 and Fe^{3+}, Ag^{+}, Zn^{2+}, Cr^{3+} and Cu^{2+} doped TiO_2 only. Cr^{3+} and Cu^{2+} doped TiO_2 was chose as the representative of the detrimental group. All the characterizations were carried out on the catalyst samples before photoreaction.

4.6.1 X-Ray Diffraction (XRD)

The crystallinity of the TiO_2 coating was identified by X-ray diffraction method employing Cu$K\alpha$ radiation. The XRD profile of undoped TiO_2 and all the doped catalysts are shown in Figure 4.5. In all the samples there exist a broad peak centered at $2\theta = 20.5°$ due to Si substrate from the glass support. A sharp peak at $2\theta = 25.4°$ can be attributed to anatase TiO_2 according to the standard pattern of anatase TiO_2. In addition to the diffraction peaks for anatase, there were no extra detectable peaks for the TiO_2 rutile phase in most of the thin films. In this study small rutile peak at $2\theta = 27.5°$ can be observed only in the XRD profile of Cr^{3+} and Co^{2+}. From the photodegradation measurements conducted, TiO_2 doped with these ions shows low photoreactivity. Therefore, the existence of rutile phase in TiO_2 can significantly reduced the photocatalytic activity of both the doped catalysts.

The sharp peak of the anatase signal shows good crystallinity and complete transformation of the anatase phase. The size or ionic radius of the dopant ions, play a part in the choice of dopants. Evidently, the nearer the radius of a dopant ion is to the radius of the Ti^{4+} ion, the easier it is for the dopant to occupy substitutional lattice positions. However, broader anatase peaks are noticed for Cu^{2+}, Co^{2+}, Zn^{2+}, and Mn^{2+} doped TiO_2 thin films. The larger peak widths indicate lower crystallinity.

The ionic radius of Cu^{2+}, Co^{2+}, Zn^{2+}, and Mn^{2+} are 72pm, 72pm, 74, and 80pm respectively, which is larger than Ti^{4+}. Therefore incorporation of transition metal ions with larger ionic radius than the host may affect the crystallinity of the anatase phase. However the XRD peak observed for Ag^{+} was sharp even though Ag^{+} have an ionic radius of 136 pm. During catalyst preparation, Ag^{+} ions would not enter the lattice of anatase phase and during the calcinations process the Ag^{+} ions would gradually migrate from the volume of TiO_2 grains to the surface of TiO_2. This caused the TiO_2 host to have a more perfect anatase structure.

XRD also did not detect the dopant phase. This could be due to the low concentration of the dopants. Tseng et al. (Tseng, 2002) observed two small Cu diffraction peaks near 2θ = 43.3 and 52° on 6.7 wt.% Cu/TiO_2 but no peaks was observed on 2.0 wt.% Cu/TiO_2. This was attributed to the low Cu loading or extremely small Cu clusters. Thus no dopants peak can be observed in this research where the dopants concentration is less than 0.3%. No dopant peak in the XRD pattern can also be attributed to the possible incorporation of dopant within the anatase lattice or the dopants could exist as a dispersed state in the TiO_2. Zhu (2000) also made a similar observation with TiO_2 film doped with Pt and Pd.

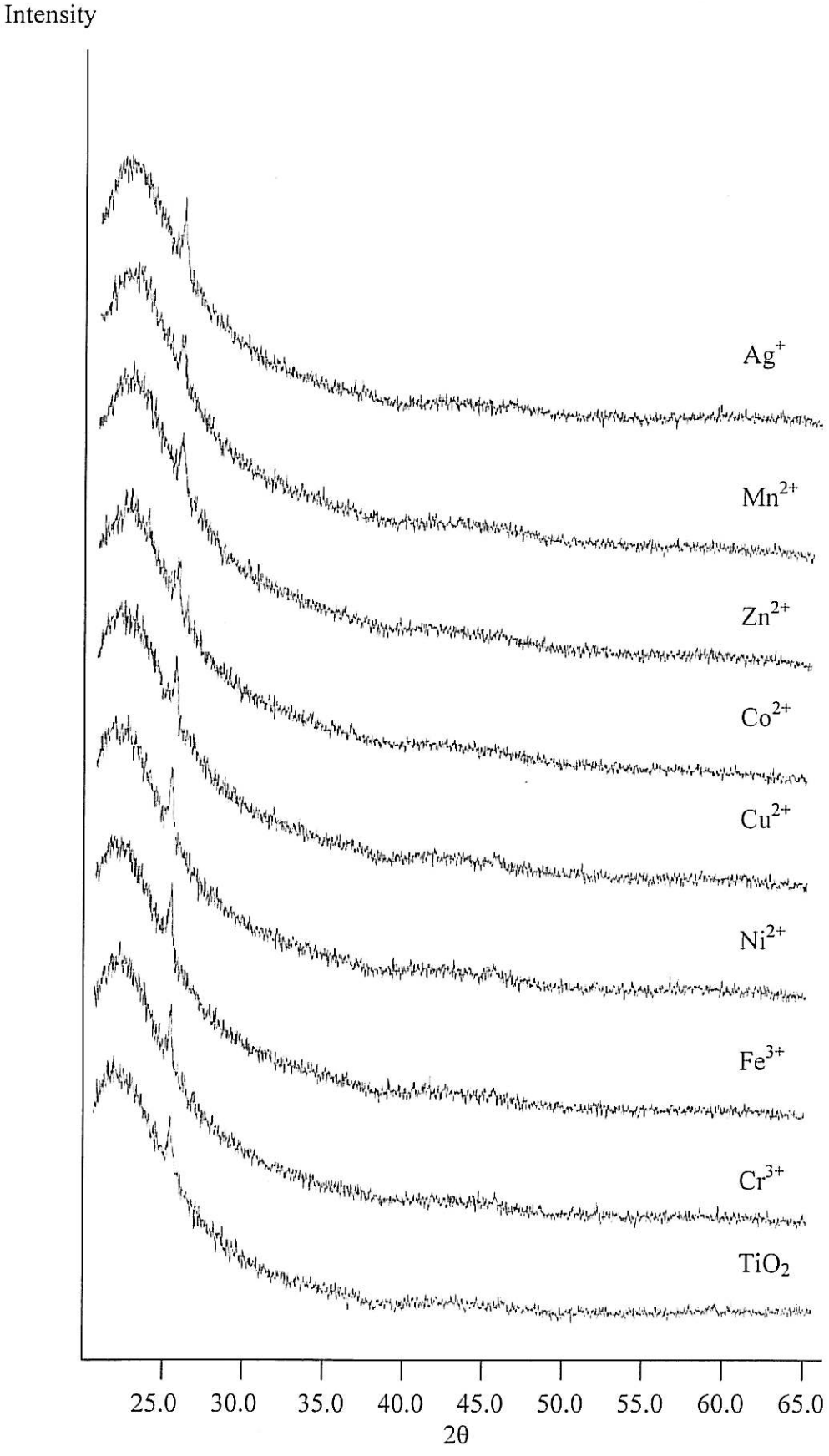

Figure 4.5: XRD profile of pure TiO_2 and doped TiO_2 thin film

4.6.2 X-ray Photoelectron spectroscopy (XPS)

Chemical composition of the thin films were determined using XPS. Characterization was conducted on undoped TiO_2, TiO_2 doped with Zn^{2+}, Fe^{3+}, and Ag^{+}. These samples were chose as they were the best catalyst for the photocatalytic oxidation of the VOCs studied. XPS was also conducted using Cr^{3+} and Cu^{2+} doped TiO_2 as the representative of the detrimental group. Table 4.9 and 4.10 show the corrected binding energy (BE) of Ti and O for undoped catalyst and samples doped with Fe^{3+}, Ag^{+} and Zn^{2+} respectively. The binding energies were calibrated with reference to C 1s at 284.5 eV for adventitious hydrocarbon contamination.

Table 4.9: Binding energy (eV) for Ti 2p in undoped and doped catalysts

Catalyst	Ti $2p_{3/2}$	Ti $2p_{1/2}$	FWHM	ΔE (eV)	Peak Area	Assignment
TiO_2	459.4	465.0	1.522	5.663	79.949	TiO_2 (anatase)
TiO_2/Fe^{3+}	459.3	464.9	1.324	5.635	69.129	TiO_2 (anatase)
TiO_2/Ag^{+}	459.1	464.8	1.360	5.688	72.836	TiO_2 (anatase)
TiO_2/Zn^{2+}	459.2	464.9	1.320	5.710	73.818	TiO_2 (anatase)

Table 4.10: Binding energy (eV) for O 1s in undoped and doped catalysts

Catalyst	O $1s_1$ (Ti-O)	Peak area	O $1s_2$ (-OH)	Peak Area	O $1s_3$ (H_2O)	Peak Area
TiO_2	530.6	163.235	532.6	162.206	533.9	58.044
TiO_2/Fe^{3+}	530.6	151.636	532.7	88.659	533.9	32.291
TiO_2/Ag^{+}	530.3	171.583	532.3	137.119	533.6	47.879
TiO_2/Zn^{2+}	530.4	158.897	532.4	97.910	533.8	36.649

For all the samples, as depicted in Table 4.9, the Ti 2p region is composed of two symmetric peaks. The Ti $2p_{3/2}$ and Ti $2p_{1/2}$ peaks, situated at a binding energy of 459.2 eV and 465.3 eV respectively, are assigned to Ti^{4+} valence state of stoichiometric anatase TiO_2. The existence of anatase was also confirmed from the XRD profiles of the thin films. These values are the same as those of pure titania and this indicates the

integrity of the TiO_2 structure, which was not greatly modified by the introduction of dopants.

In Table 4.10, it can be seen clearly that the O 1s region can be resolved into three peaks. The dominant peak centered at 530.6 eV is characteristic of metallic oxides, which is in agreement with O 1s electron binding energy for TiO_2 (Ti^{4+} - O). This peak was also observed in all the doped TiO_2 catalysts. The peak at 532.6 eV may be attributed to the surface hydroxyl group existed from chemically adsorbed H_2O forming Ti-OH. The existence of the metallic oxide and surface hydroxyl peaks is in agreement with the work of Kumar (2000) where non-crystalline TiO_2 thin film coated on silicon substrate was prepared using sol from organic medium.

The peak situated at 533.9 eV is due to physically absorbed H_2O on TiO_2. The surface hydroxyl groups can play an important role in the photocatalytic reactions because the photoinduced holes can attack the surface hydroxyl and yield surface bound OH radical with high oxidation capability thus enhance the thin film photocatalytic activity. Therefore although the amount of this species is relatively small as compared to the chemically absorbed water, it is enough to significantly increase the photocatalytic activity of TiO_2 and thus the rate of VOCs degradation.

4.6.3 Scanning Electron Microscopy (SEM)

Figure 4.6 shows the SEM micrograph for undoped TiO_2. All the other catalyst has a similar surface morphology. All scans were made with 10k magnification and 20 kV or 12 kV scanning voltage. There are homogeneously distributed fine pores in all the coatings. Yu (Yu, 2001) also observed a similar SEM image of TiO_2 thin films prepared from alkoxide solutions containing polyethylene glycol by the sol-gel method on soda glass. The pore size was observed to increase with increasing dopant ionic radius. TiO_2 doped Zn^{2+} have the largest pore size and is inhomogeneously and unevenly distributed. A close look at the micrograph of TiO_2/Zn^{2+} thin film reveals the agglomeration process has occurred.

Pores are produced in the thin films because PEG contained in the gel coating films decomposes completely at 600 °C (Yu, 2001). The size of the pores was also related to the size of the metal ions doped into TiO_2. As the size of the metal ions becomes bigger, the pore size also increases. However for Ag^+, because the radius of Ag^+ (126 pm) is much larger than that of Ti^{4+} (68 pm), Ag^+ ions introduced by the sol-gel process would not enter the lattice of anatase phase to form a stable solid solution. During the calcinations process these uniformly dispersed Ag^+ ions would gradually migrate from the volume of TiO_2 grains to the surface of TiO_2 causing a decrease in the pore size.

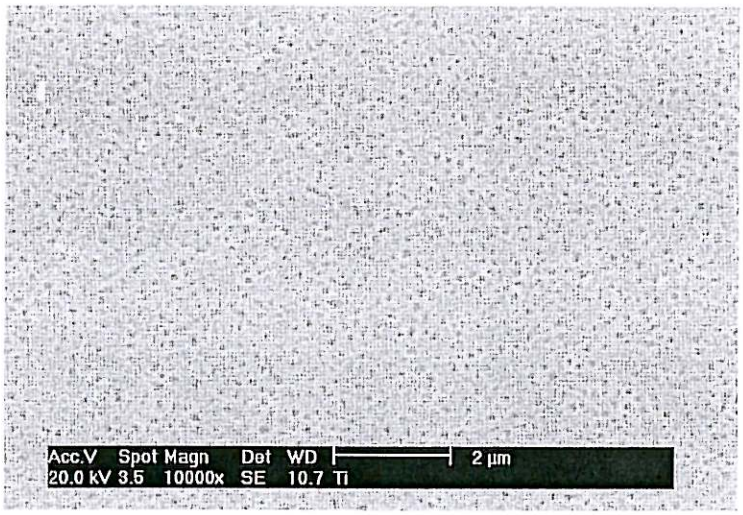

Figure 4.6: SEM micrograph of undoped TiO_2 thin film

All dopants, which were not detectable in the XRD and XPS analysis, were observed by EDAX. A homogeneous dispersion of metal ions throughout the film was shown by multiple spots analysis with a 1 µm spot size on all the doped films.

4.6.4 UV-Vis Spectroscopy

TiO_2 and TiO_2 doped with Zn^{2+}, Fe^{3+} and Ag^+ have the highest absorbance (~ 40%) at the visible region (Figure 4.7). Since these doped thin films can absorbed light in a wider range of wavelength and utilize more light energy than the TiO_2 thin film, it follows that a higher photocatalytic activity should be expected in the thin film.

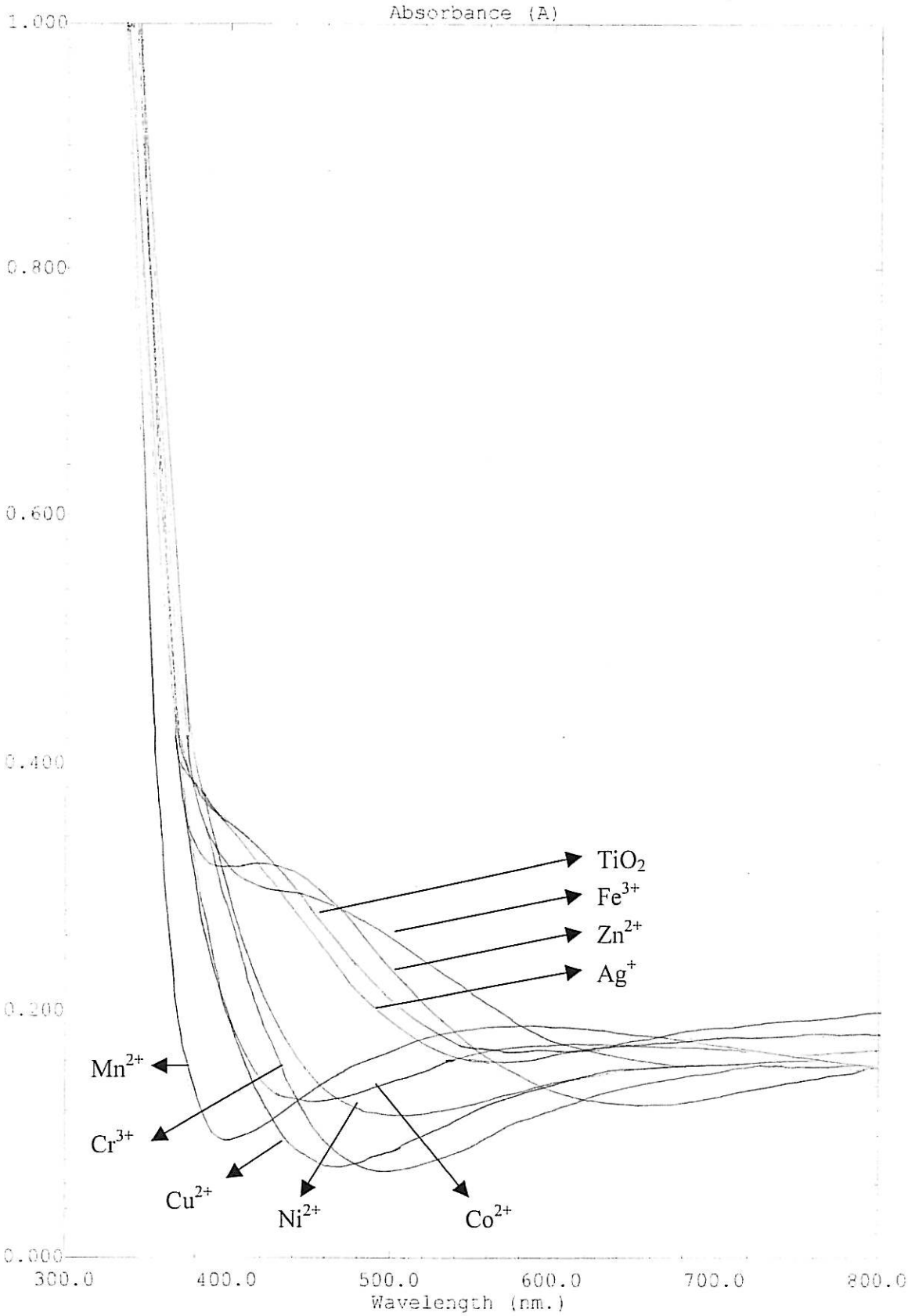

Figure 4.7: UV-Vis absorption spectra for doped and undoped thin film

A slight shift to a higher wavelength or red shift was noted for Cr^{2+}, Ni^{2+}, Co^{2+}, Cu^{2+} and Fe^{3+}. This indicates a decrease in the band gap of TiO_2 as it is doped with the respective dopants. Mn^{2+}, Ag^{+} and Zn^{2+} doped TiO_2 showed a significant blue shift to a shorter wavelength showing an increased band gap value. The absorption spectrum for Zn^{2+} and Fe^{3+} also showed a marked absorption at 380 – 500nm region that was higher than the pure TiO_2. A similar absorption at 450 – 800 nm but with lower intensity was also observed for Mn^{2+}, Cr^{3+}, Co^{2+}, Cu^{2+} and Ni^{2+}. These absorption bands could be ascribed to the charge transfer transition, which may be alternatively described as excitation of an electron of metal ions into the conduction band of TiO_2 (Malati, 1986).

The red shift in optical energy gap could be due to the below factors. The energy level for dopants lies below the conduction band edge (E_{cb}) and above valence band edge (E_{vb}) of TiO_2. Introduction of such energy levels in the band gap induces the red shift in the band gap transition and the visible light absorption through a charge transfer between a dopant and CB (or VB) or a d-d transition in the crystal field according the energy level (Hoffmann, 1995). A red shift in the absorption edge also indicates that the TiO_2 film is modified to absorb visible light by doping. This is in agreement with the results of Cr doped TiO_2 (Herrmann, 1984; da Silva, 2002), Co doped TiO_2 (Haro-Poniatowski, 1996) and Fe doped TiO_2 thin film (Gracia, 2002; Jiang, 2003).

CHAPTER V

5.0 CONCLUSION

TiO_2 thin film with high photocatalytic activity was successfully prepared in this study using the sol-gel and dip-coating methods. The thin film prepared was transparent, robust, non-abrasive and show high photoreactivity in the photodegradation of benzene, toluene, acetone, *m*-xylene and tetrachloroethylene. Addition of dopants into TiO_2 was conducted in the effort to increase the efficiency of the catalyst. Several conclusions can be made from the research conducted.

1. The photodegradation rate of a volatile organic compound using metal ions doped TiO_2 could have a positive or negative effect depending on the kind and concentration of the metal ions.
2. The same metal ion was observed to give a different effect on the photodegradation rate of different organic compound. Different concentration of organic compound may also influence the activity of the doped TiO_2.
3. Cu^{2+}, Co^{2+}, Cr^{3+}, Ni^{2+} and Mn^{2+} are detrimental to the photoactivity of TiO_2 with all organic compounds investigated.
   Zn^{2+} increased the activity of TiO_2 in toluene and *m*-xylene degradation.
   Fe^{3+} and Ag^{+} are the most photoactive system in the photooxidation of benzene.
   Fe^{3+} increased the activity of TiO_2 in the degradation of acetone of higher concentration.
4. The kinetics of the organic compounds degradation was well described by the Langmuir-Hinshelwood rate forms. The degradation rate is dependent on K and k. However a higher adsorption constant may not result in a higher degradation rate.
5. The high photodegradation of TeCE compared to non-chlorinated hydrocarbon was due to a chain mechanism involving chlorine radical.
6. Characterizations on the thin films shows that:

- the TiO_2 are primarily anatase phase.
- the film consisted of fine pores that are homogeneously distributed on the surface.
- the catalyst with the best photocatalytic activity contained Ti^{4+}, chemically and physically adsorbed water. While the "*bad catalyst*" contained Ti^{3+} and a lower quantity of physically adsorbed water.
- the adsorption edge of Cr^{2+}, Ni^{2+}, Co^{2+}, Cu^{2+} and Fe^{3+} shifted slightly to a higher wavelength. This indicates a decrease in the band gap of TiO_2 as it is doped with the respective dopants. Mn^{2+}, Ag^{+} and Zn^{2+} doped TiO_2 showed a significant shift to a shorter wavelength showing an increased band gap value.
- Structural and optical charaterization of the catalysts using methods such as XRD, SEM/EDAX, XPS and UV-Vis has shown that the crystal structure, the type of species found on the catalyst surface, porosity, surface area and band gap play an important role in increasing the photocatalytic reactivity of TiO_2.

CHAPTER VI

6.0 FUTURE WORKS

Heterogeneous photocatalysis on TiO_2 has been shown to provide an effective method to degrade organic pollutants from gaseous streams. Addition of dopants into TiO_2 matrix significantly increased its photocatalytic activity. In this study benzene, toluene, acetone, *m*-xylene and tetrachloroethylene has high rate of photocatalytic oxidation using doped TiO_2. About 100% of benzene and acetone conversion was observed using Fe^{3+} and Ag^{+} doped TiO_2 compared to the pure catalyst while the photodegradation of toluene and *m*-xylene was greatly enhanced using Zn^{2+} doped TiO_2. Although positive results was obtained from this study, more and in depth work must be conducted to answer questions that have arisen through the course of this work. The answers gathered could then be used to understand and complete the overall picture of heterogeneous photocatalytic oxidation of VOCs using TiO_2.

1. Determining the quantum yield (QY) of the photocatalytic oxidation of VOCs using *chemical actinometers* such as ferrioxalate $[Fe(C_2O_4)_3]^{3+}$, Reinecke's salt $[Cr(NH_3)_2(SCN)_4]$ and Aberchrome 540. The value of QY obtained will represent the effectiveness of the catalyst in degrading environmental pollutants.

2. In this study the existence of dopant ions was detected using EDAX and chromium was the only metal ion detected by XPS. Therefore, in order to obtain more accurate information about the existence and stoichiometry of the catalyst Auger Electron Spectroscopy (AES) and Secondary Ion Mass Spectroscopy (SIMS) could be perform respectively.

3. The use of HPLC or *in situ* FT-IR spectroscopy could be an alternative method to identify the intermediates and products formed. In depth study of the reactive species

References

Augugliaro, V., Voluccia, S., Loddo, V., Marchese, L., Martra, G., Palmisano, L. and Schiavello, M. (1999). "Photocatalytic oxidation of gaseous toluene on anatase TiO_2 catalyst: mechanistic aspects and FT-IR investigation." *Applied Catalysis B: Environmental.* **20**. 15-27

Avila, P., Bahamonde, A., Blanco, J., Sanchez, B., Cardona, A.I. and Romero, M. (1998). "Gas-phase photo-assisted mineralization of volatile organic compounds by monolithic titania catalyst." *Applied Catalysis B: Environmental.* **17**. 75-88.

Bahnemann, D.W., Monig, J. and Chapman, R. (1987). "Efficient Photocatalysis of the Irreversible One-Electron and Two-Electron Reduction of Haloethane on Platinized Colloidal Titanium Dioxide in Aqueous Suspension." *Journal of Physical Chemistry*. **91**. 3782-3788.

Brickley, R.I., Munuera, G. and Stone, F.S. (1973). "Photoadsorption and photocatalysis at rutile surface II: Photocatalytic oxidation of isopropanol." *Journal of Catalysis*. **31**. 398-407.

Brinker, C.J. and Hurd, A.J. (1991). "Sol-gel thin film formation." *The Ceramic Society of Japan.* **99**. 862-877.

Borgarello, E., Kiwi, J., Gratzel, M., Pelizzetti, E. and Visca, M. (1982). "Visibble light induced water cleavage in colloidal solutions of chromium-doped titanium dioxide particles." *J. Am. Chem. Soc.* 104, 2996-3002.

Burr, M.L. (1995). "Pollution: does it cause asthma?" *Archives of Disorders in Childhood.* **72**. 377-387.

Choi, W., Termin, A. and Hoffman, M.R. (1994). "The Role of Metal Ion Dopants in Quantum-Sized TiO_2: Correlation between Photoreactivity and Charge Carrier Recombination Dynamics." *Journal of Physical Chemistry*. **98**. 13669-13679.

D'Hennezel, O., Pichat, P. and Ollis, D.F. (1998). "Benzene and toluene gas-phase photocatalytic degradation over H_2O and HCl pretreated TiO_2: by-products and mechanism." *Journal of Photochemistry and Photobiology A: Chemistry.* **118**. 197-204

Da Silva, R.C., Alves, E. and Cruz, M.M. (2002). "Conductivity behaviour of Cr implanted TiO_2." *Nuclear Instruments and Methods in Physics Research B.* **191**. 158-162.

Dibble, L.A., and Raupp, G.B. (1990). "Kinetics of the gas-solid heterogeneous photocatalytic oxidation of trichloroethylene by near UV illumination TiO_2." *Catalysis Letter.* **4**. 345-354.

Di Paola, A., Gracia-Lopez, E., Ikeda, S., Marci, G., Ohtani, B. and Palmisano, L. (2002). "Photocatalytic degradation of organic compounds in aqueous systems by transition metal doped polycrystalline TiO_2." *Catalysis Today.* **75**. 87-93.

Dvoranova, D., Brezova, V., Mazuir, M. and Malati, M.A. (2002). "Investigations of metal-doped titanium dioxide photocatalysts." *Applied Catalysis B: Environmental.* **37**. 91-105.

Fox, M.A. and Dulay. M.T. (1993). "Heterogeneous Photocatalysis." *Chemical Review.* **93**. 341-357.

Fu, X., Zeltner, W.A. and Anderson, M.A. (1995). "The Gas Phase Photocatalytic Mineralization of Benzene on Porous Titania-Based Catalyst." *Applied Catalyst B: Environmental.* **6**. 209-224.

Fujishima, K., Hashimoto, K. and Watanabe, T. (1999). "TiO_2 Photocatalysis: Fundamentals and Applications." BkC, Inc., Tokyo. p15

Gracia, F., Holgado, J.P., Yubero, F. and Gonzales-Elipe, A.R. (2002). "Phase mixing in Fe/TiO_2 thin films prepared by ion beam-induced chemical vapour deposition:

optical and structural properties." *Surface and Coatings Technology*. **158-159**. 552-557.

Gratzel, M. and Howe, R.F. (1990). "Electron Paramagnetic Resonance (EPR) Studies of Doped TiO_2 Colloids." *J. Phys. Chem.* **94**. 2566-2572.

Haro-Poniatowski, E., Vargas-Munos, S., Arroyo-Murillo, R., Rodriguez-Talavera, R. and Diamant, R. (1996). "Laser-induced crystallization of Co(II)-doped titania." *Materials Research Bulletin*. **31**. 329-334.

Herrmann, J.M., Disdier, J., Mozzanega, M-N. and Pichat, P. (1979). "Heterogeneous Photocatalysis: In situ photoconductivity study of TiO_2 during oxidation of isobutane into acetone." *J. Catalysis*, **60**. 369-377

Herrmann, J-M., Disdier, J. and Pichat, P. (1984). "Effect of Chromium Doping on the Electrical and Catalytic Properties of Powder Titania Under UV and Visible Illumination." *Chemical Physics Letter*. **108**. 618-622.

Hoffman, M.R., Martin, S.T. and Choi, W. (1995). "Environmental Applications of Semiconductor Photocatalysis." *Chemical Review*. **95**. 69-96.

Hong, A.P., Bahnemann, D.W. and Hoffmann, M.R. (1987). "Cobalt (II) Tetrasulfophthalocyanine on titanium dioxide: A new efficient electron relay for the photocatalytic formation and depletion of hydrogen peroxide in aqueous suspension." *J. Phys. Chem.* **91**. 2109-2117.

Jacoby, W.A., Blake, D.M., Noble, R.D. and Koval, C.A. (1995). "Kinetics of the Oxidation of Trichloroethylene in Air via Heterogeneous Photocatalysis." *Journal of Catalysis*. **157**. 87-96.

Jiang, H. and Gao, L. (2003). "Enhancing the UV inducing hydropholicity of TiO_2 thin film by doping Fe ions." *Materials Chemistry and Physics*. **77**. 878-881.

Jones, A.P. (1999). "Indoor air quality and health." *Atmospheric Environment*. **33**. 4535-4564.

Karakitsou, K.E. and Verykios, X.E. (1993). "Effects of Altervalent Cation Doping on TiO_2 on its Performance as a Photocatalyst for Water Cleavage." *Journal of Physical Chemistry*. **97**. 1184-1189.

Kim, D.H. and Anderson, M.A. (1996). "Solution factors affecting the photocatalytic and photoelectrocatalytic degradation of formic acid using supported TiO_2 thin films." *Journal of Photochemistry and Photobiology A: Chemistry*. **94**. 221-229.

Kumar, P.M., Badrinarayanan, S. and Sastry, M. (2000). "Nanocrystalline TiO_2 studied by optical, FTIR and X-ray photoelectron spectroscopy: correlation to presence of surface states." *Thin Solid Films*. **358**. 122-130.

Lipfert, F.W. (1997). "Air pollution and human health: perspective for the '90s and beyond." *Risk analysis*. **17**. 137-146.

Litter, M.I. and Navio, J.A. (1996). "Photocatalytic Properties of Iron-Doped Titania Semiconductor." *Journal of Photochemistry and Photobiology A: Chemistry*. **98**. 171-181.

Malati, M.A. and Wong, W.K. (1984). "Doping TiO_2 For Solar Energy Applications." *Surface Technology*. **22**. 305-322.

Martin, S.T., Morrison, C.L and Hoffman, M.R. (1994). "Photochemical Mechanism of Size-Quantized Vanadium Doped TiO_2 Particles." *Journal of Physical Chemistry*. **98**. 13695-13704.

Morrison, R.T. and Boyd, R.N. (1987). "Organic Chemistry." 5^{th} edition. Boston, MA. Allyn and Bacon. 886.

Moser, J., Gratzel, M. and Gallay, R. (1987). "Inhibition of Electron-Hole Recombination in Substitutionally Doped Colloidal Semiconductor Crstallites." *Helvetica Chimica. Acta.* **70**. 1596-1604.

Navio, J.A., Colon, G., Litter, M.I. and Bianco, G.N. (1996). "Synthesis, Characterization and Photocatalytic Properties of Iron-Doped Titania Semiconductor Prepared from TiO_2 and Iron (III) acetylacetonate." *J. Molecular Catalysis A: Chemical.* **106**. 267-276.

Nimlos, M.R., Jacoby, W.A., Blake, D.M. and Milne, T.A. (1993). "Direct Mass Spectroscopy Studies of the Destruction of Hazardous Wastes. 2. Gas-Phase Photocatalytic Oxidation of Trichloroethylene over TiO_2: Products and Mechanisms." *Environmental Science and Technology.* **27**. 732-740.

Norback, D., Bjornsson, E., Janson, C., Widstrom, J. and Boman, G. (1995). "Asthma and indoor environment: the significance of emission of formaldehyde and volatile organic compounds from newly painted indoor surfaces." *Occupational and Environmental Medicine.* **52**. 388-395.

Palmisano, L, Augugliaro, V., Sclafani, A. and Schiavello, M. (1988). "Activity of Chromium-Ion-Doped Titania for the Dinitrogen Photoreduction to Ammonia and for Phenol Photodegradation." *Journal of Physical Chemistry.* **92**. 6710-6713.

Park, D.R., Zhang. J.L., Ikene, K., Yamashita. H., and Anpo, M. (1999). "Photocatalytic oxidation of ethylene to CO_2 and H_2O on ultrafine powdered TiO_2 photocatalysts in the presence of O_2 and H_2O." *Journal of Catalysis.* **185.** 114-119.

Peral, J., and Ollis, D.F. (1992). "Heterogeneous photocatalytic Oxidation of Gas-phase Organics for Air Purification: Acetone, 1-Butanol, Butyraldehyde, Formaldehyde." *Journal of Catalysis.* **136**. 554-565.

Radecka, M., Zakrzewska, K., Wierzbicka, M., Gorzkowska, A. and Komornicki, S. (2002). "Study of the TiO_2-Cr_2O_3 system for photoelectrolytic decomposition of water." *Solid State Ionics.* In press

Ranjit, K.T. and Viswanathan, B. (1997). "Synthesis, Characterization and Photocatalytic of Ion Doped TiO_2 Catalysts." *J. Photochem. Photobiol. A: Chem.*, **108**. 79-79

Rothenberger, G., Moser, J., Gratzel, M., Serpone, N. and Sharma, D.K. (1985). "Charge Carrier Trapping and Recombination Dynamics in Small Semiconductor Particles." *Journal of American Chemical Society*. **107**. 8054-8059.

Sanhueza, E., Hisatsune, I.C. and Heicklen, J. (1976). "Oxidation of haloethylenes." *Chemical Reviews*. **76**. 801-826.

Sauer, M.L., and Ollis, D.F. (1994). "Acetone Oxidation in a Photocatalytic Monolith Reactor." *Journal of Catalysis*. **149**. 81-91.

Sawyer, R.F., Harley, R.A., Cadle, S.H., Norbeck, J.M., Slott, R. and Bravo, H.A.. (2000). "Mobile sources critical review: 1998 NARSTO Assessment." *Atmospheric Environment*. **34**. 2161-2181.

Schrauzer, G.N. and Guth, T.D. (1977). "Photolysis of Water and Photoreduction of Nitrogen on Titanium Dioxide." *Journal of the American Chemical Society*. **99**. 7188-7193.

Soria, J., Conesa, J.C., Augugliaro, V., Palmisano, L., Schiavello, M. and Sclafani, A. (1991). "Dinitrogen Photoreduction to Ammonia over Titanium Dioxide Powders Doped with Ferric Ions." *J. Phys. Chem.* **95**. 274-282.

Tseng, I-Hsiang, Chang, Wan-Chen, Wu and Jeffrey C.S. (2002). "Photoreduction of CO_2 using sol-gel derived titania and titania-supported copper catalysts." *Applied Catalysis B: Environmental*. **37**. 37-48.

Vrachou, E., Gratzel, M. and McEvoy, A.J. (1989). "Efficient visible light photoresponse following surface complexation of titanium dioxide with transition metal cyanides." *J. Electroanl. Chem.* **258**. 193-205.

Wallace, L.A. (1991). "Comparison of risks from outdoor and indoor exposure to toxic chemicals." *Environmental Health Perspectives*. **95**. 7-13.

Wang, Y., Cheng, H., Hao, Y., Ma, J., Li, W. and Cai, S. (1999). "Photoelectrochemical properties of metal-ion-doped TiO_2 nanocrstalline electrodes." *Thin Solid Films*. **349**. 120-125.

Wilke, K. and Breuer, H.D. (1999). "The influence of transition metal doping on the physical and photocatalytic properties of titania." *Journal of Photochemistry and Photobiology A: Chemistry*. **121**. 49-53.

Xu, A-W., Gao, Y. and Liu, H-Q. (2002). "The preparation, characterization and their photocatalytic activities of rare-earth-doped TiO_2 nanoparticles." *J. Catalysis*. **207**. 151-157.

Xu, W. and Raftery, D. (2001). "In Situ Solid-state Nuclear Magnetic Resonance Studies of Acetone Photocatalytic Oxidation on Titanium Oxide Surfaces." *Journal of Catalysis*. **204**. 110-117.

Yamazaki-Nishida, Fu, X., Anderson, M.A. and Hori, K. (1996). "Chlorinated byproducts from the photoassisted catalytic oxidation of trichloroethylene and tetrachloroethylene in the gas phase using porous TiO_2 pellets." *Journal of Photochemistry and Photobiology A: Chemistry*. **97**. 175-179.

Yu, J., Zhao, X., Zhao, Q. and Wang, G. (2001). "Preparation and characterization of super-hydrophilic porous TiO_2 coating films." *Materials Chemistry and Physics*. **68**. 253-259.

Yuan, Z., Jia, J. and Zhang, L. (2002). "Influence of co-doping of Zn(II) + Fe(III) on the photocatalytic activity of TiO_2 for phenol degradation." *Materials Chemistry and Physics*. **73**. 323-326.

Zhu, Y., Zhang, L., Yao, W. and Cao, L. (2000). "The chemical states and properties of doped TiO_2 film photocatalyst prepared using the sol-gel with $TiCl_4$ as a precursor." *Applied Surface Science*. **158**. 32-37.

Appendix 1: Calibration Graphs for the VOCs.

Figure 1.1: Calibration Graph for Benzene

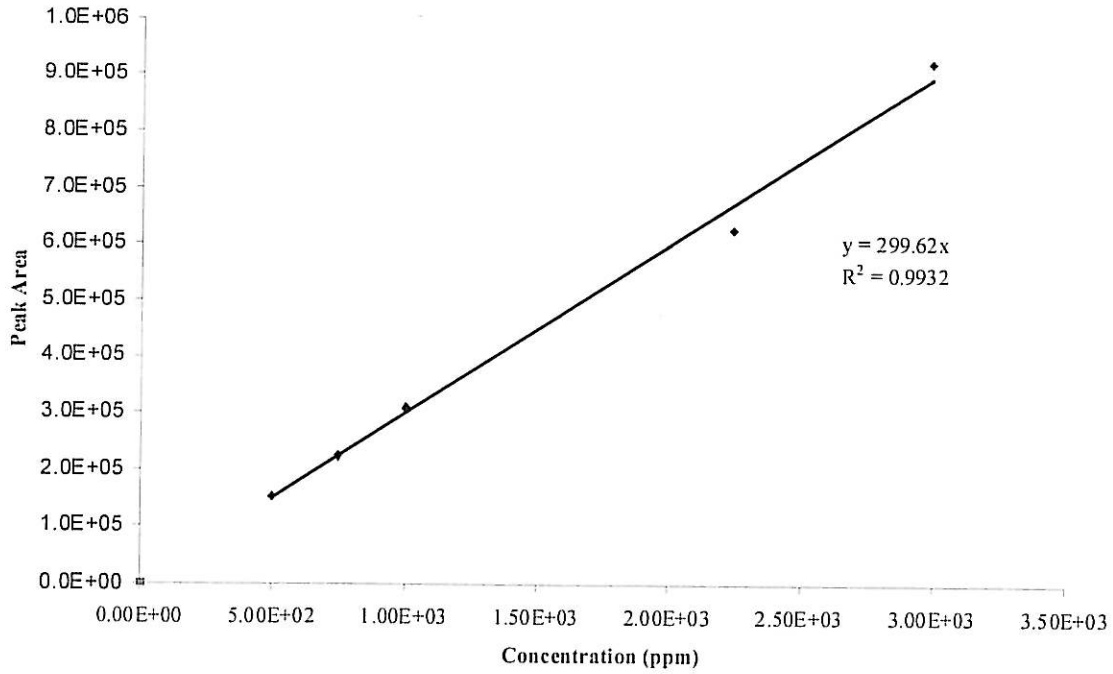

Figure 1.2: Calibration Graph for Toluene

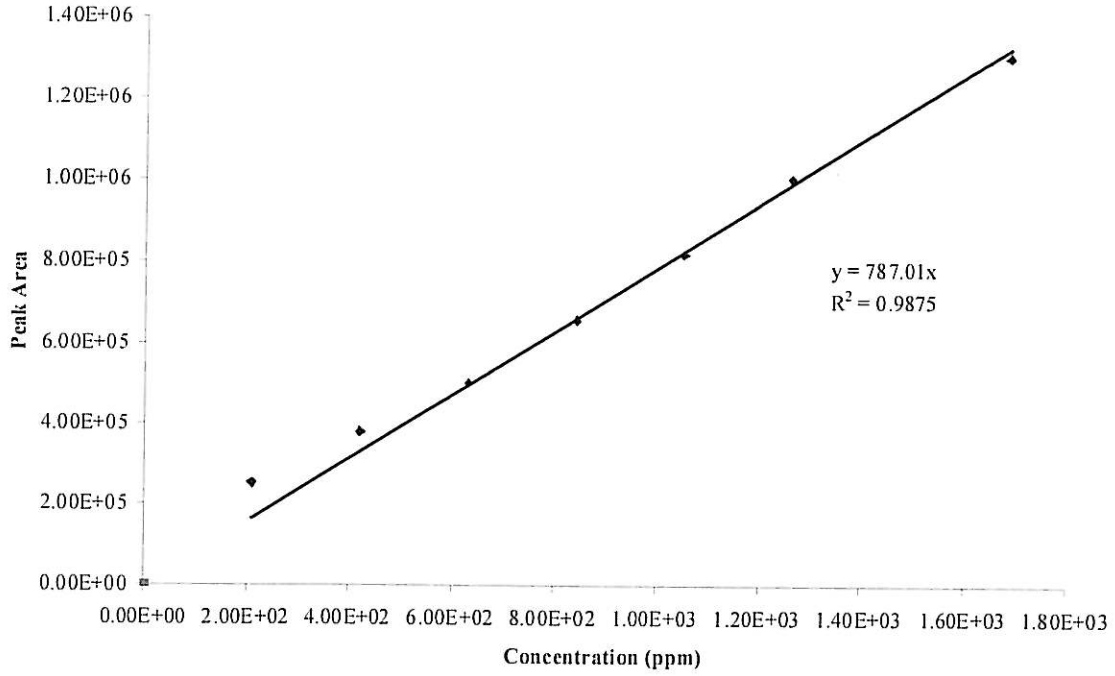

Figure 1.3: Calibration Graph for Acetone

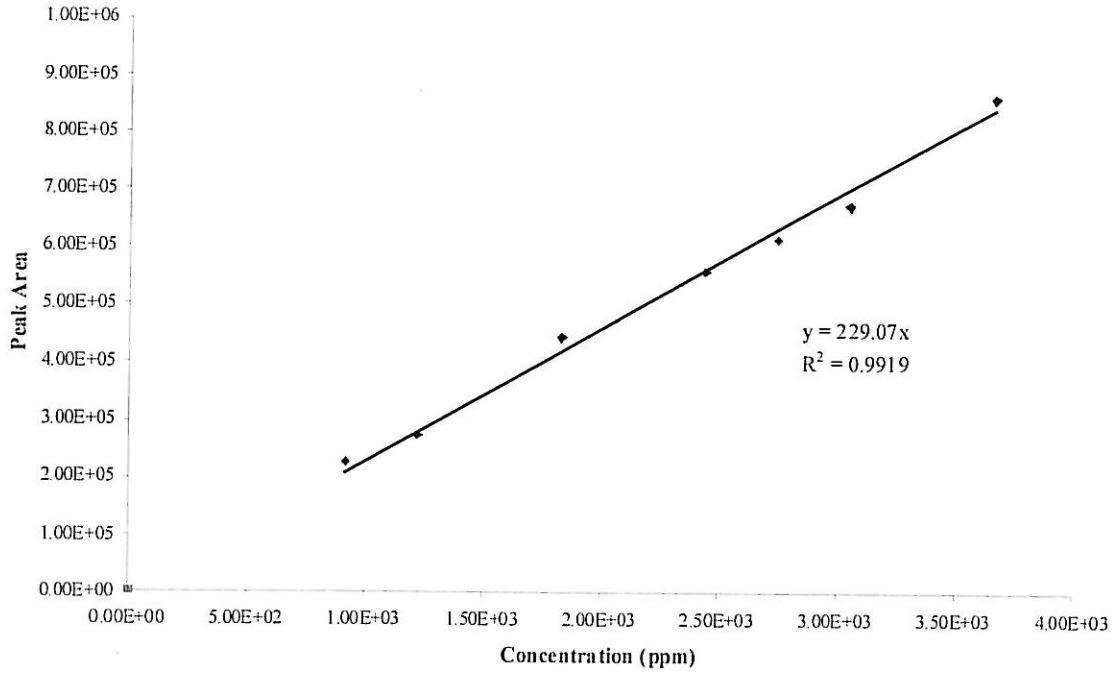

Figure 1.4: Calibration Graph for *m*-Xylene

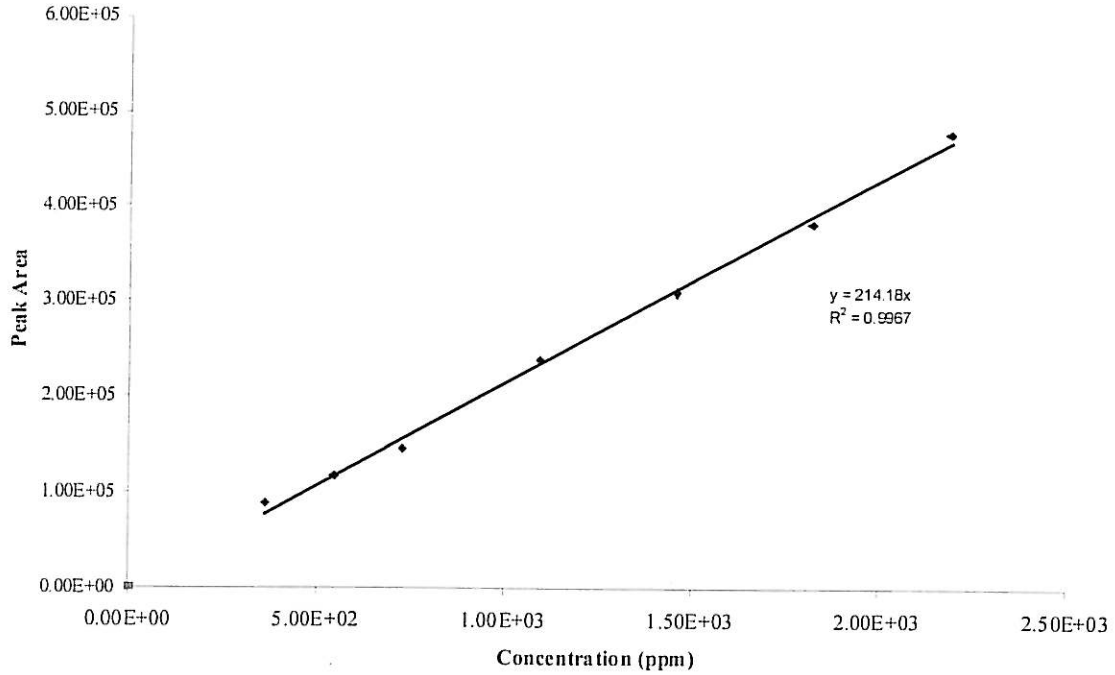

Figure 1.5: Calibration Graph for Tetrachloroethylene